UNCLASSIFIED

AD NUMBER
AD826980
LIMITATION CHANGES
TO: **Approved for public release; distribution is unlimited.**
FROM: **Distribution authorized to U.S. Gov't. agencies and their contractors; Critical Technology; JAN 1968. Other requests shall be referred to Air Force Flight Dynamics Laboratory, Attn: FDTR, Wright-Patterson AFB, Ohio 45433. This document contains export-controlled technical data.**
AUTHORITY
AFFDL ltr, 31 May 1973

THIS PAGE IS UNCLASSIFIED

AFFDL-TR-67-122

A CLIMATOLOGICAL-WIND TURBULENCE MODEL FOR ESTIMATING LOW ALTITUDE GUST LOADS

U. OSCAR LAPPE

NEW YORK UNIVERSITY

TECHNICAL REPORT AFFDL-TR-67-122

JANUARY 1968

This document is subject to special export controls and each transmittal to foreign governments or foreign nationals may be made only with prior approval of Air Force Flight Dynamics Laboratory, FDTR, Wright-Patterson Air Force Base, Ohio 45433.

AIR FORCE FLIGHT DYNAMICS LABORATORY
AIR FORCE SYSTEMS COMMAND
WRIGHT-PATTERSON AIR FORCE BASE, OHIO

72

NOTICE

2

200 - January 1968 - CO455 - 23-509

A CLIMATOLOGICAL-WIND TURBULENCE MODEL FOR ESTIMATING LOW ALTITUDE GUST LOADS

U. OSCAR LAPPE

FOREWORD

This report was prepared by the Research Division of the School of Engineering and Science of New York University, in Air Force Contract AF 33(615)-2566, under Task No. 136702 of Project No. 1367. The work was administered under the direction of Structures Division of Air Force Flight Dynamics Laboratory. Mr. Paul Hasty was Project Engineer for the Laboratory. This report was submitted March 30, 1967 for publication.

The studies presented in this report cover the period of 15 April 1965 to 15 October 1966. The study was conducted by the Geophysical Sciences Laboratory of the Department of Meteorology and Oceanography of New York University (2455 Sedgwick Avenue, Bronx, New York 10468). The work was under the supervision of Project Director, U. Oscar Lappe. Mr. Peter Ronberg assisted in the project activities reported herein. The illustrations were prepared by Mrs. Gertrude Fisher and the typing was performed by Mrs. Lillian Bloom.

This report is the final report and concludes the work on Contract AF 33(615)-2566. The contractor's report number is Geophysical Sciences Laboratory report number 66-13.

This technical report has been reviewed and is approved.

Francis J. Janik, Jr.
Chief, Theoretical Mechanics Branch
Structures Division

ABSTRACT

The final phase in the development of a low altitude turbulence model for aircraft gust load application is described. The basic data used for this model are the B-66B low-level gust data and climatological wind data provided by the National Weather Records Center, Asheville, N.C. In preceding studies the turbulence spectrum functions, rms gust velocity/mean wind speed functions, and mean wind speed distribution functions were determined for variations in height, atmospheric stability, and terrain roughness conditions. In this final study needed to complete the turbulence model, climatological wind statistics are used to relate average mean wind speed characteristics to terrain, height, thermal stability, time of day and seasonal variations. The data represent locations throughout the United States. Based on results obtained from the climatological wind statistics, procedures are outlined for applying the turbulence model to estimate aircraft gust load exceedances for a specified low altitude operational history. A preliminary comparison of the model and B-52 service load data is made for an 800 ft terrain-clearance altitude.

TABLE OF CONTENTS

NOMENCLATURE

φ	normalized spectrum function
f	frequency
k	wave number, f/U
Ω	wave number times 2π
$T(i\Omega)$	transfer function of any airplane response item to sinusoidal gust of unit amplitude
U	mean wind speed or airplane forward velocity
u	mean wind speed
$\bar{u}$	climatic-wind-speed
h, z	height above surface
σ_w	rms of vertical gust velocity
L	scale parameter
Y	general load parameter
$N(Y)$	number of exceedances of a given load
N_o	number of crossings of Y of zero reference value with a positive slope per foot distance flown
$\bar{A}^2$	integral of product of the normalized spectrum function and the square of the transfer function
H	hour of day

Section 1

INTRODUCTION

This report summarizes the final phase of a study to develop a turbulence model to relate low-level atmospheric turbulence spectra to mean meteorological parameters, terrain conditions, and height. Previous phases associated with the model development are reported in refs 1-4. The model is designed to provide a gust load procedure to account for the effects of turbulence on aircraft design load factors and for estimating structure fatigue life. The procedure requires assigning estimates of diurnal and seasonal flight operations (weights, speeds, etc) in conjunction with terrain and altitude conditions.

A summary of the previous three phases repor ed in refs 1-3 is presented below:

Ref 1: Data obtained from the B-66 low-level gust study (ref 5) were analyzed from a meteorological and a power spectral density standpoint. Meteorologically, the basic B-66 wind speed and temperature data were combined with synoptic observations to provide wind speed and lapse rate estimates consistent with both B-66 estimates and synoptic data. From the spectrum data analysis a spectral shape representation with height was obtained for two (rough and smooth) terrain classifications.

Ref 2: Relations between the standard deviation of vertical velocity and mean wind speed for smooth terrain conditions were obtained for three atmospheric stability classes; and 1400 ft tower data were analyzed to provide mean wind profile characterisics for the three lapse rate conditions.

Climatological wind statistics for Dayton, Ohio were analyzed and the possibility of obtaining a generalized mean wind distribution function based on the average climatic wind speed was suggested.

Ref 3: Climatological data for smooth and rough terrain stations were analyzed and generalized wind distribution functions were obtained. Procedures for estimating the rms gust velocity probability density distribution functions and the exceedance probability distributions were determined.

In the current final phase of the basic model development, extensive climatological data are analyzed for the purpose of (1) confirming the wind speed probability density distribution functions, and (2) providing a climatic mean wind speed model to account for diurnal and seasonal changes as related to height, atmospheric stability, and terrain conditions. In addition, step-by-step procedures are outlined for applying the turbulence model to estimate aircraft gust load exceedance probabilities.

Section 2

GENERAL APPROACH TO THE PROBLEM

A summary of the meteorological and geophysical aspects of the low altitude gust load model is described in this section.

1. Basic load expression

The basic equation, presented in refs 3 and 4, describing the average number of peak values per unit distance exceeding a given load Y is given by

$$N(Y) = N_o \int_0^\infty f(\sigma_w) \exp\left\{\frac{-Y^2}{2A^2 \sigma_w^2}\right\} d\sigma_w \tag{1}$$

where σ_w is the rms of vertical gust velocity, $f(\sigma_w)$ is the probability density function of σ_w, and N_o and A^2 are defined as

$$N_o = \frac{1}{2\pi} \left\{ \frac{\int_0^\infty \Omega^2 |T(i\Omega)|^2 \varphi_{w_N}(\Omega)\, d\Omega}{\int_0^\infty |T(i\Omega)|^2 \varphi_{w_N}(\Omega)\, d\Omega} \right\}^{\frac{1}{2}}$$

and

$$A^2 = \int_0^\infty |T(i\Omega)|^2 \varphi_{w_N}(\Omega)\, d\Omega$$

where $\varphi_{w_N}(\Omega) = \varphi(\Omega)/\sigma_w^2$ is the normalized gust spectral density function, and $T(i\Omega)$ is the airplane load response to a sinusoidal gust of unit amplitude.

To determine the load exceedance probabilities for a range of aircraft operating conditions (weight, speed, etc) and geophysical environmental conditions (wind speeds, atmospheric stability, topography, etc), it is necessary to evaluate Equation (1) for significant changes in these conditions. Thus,

$$\overline{N(Y)} = \sum \tau_{ij} \dot{N}(Y) \qquad (2)$$

where $\sum \tau_{ij} = 1$ and $\overline{N(Y)}$ is the load exceedance probability averaged over conditions ij.

2. Basic approach

The basic approach to the low level gust procedure involves modeling the vertical gust velocity intensity (σ_w) and spectrum characteristics (φ_{w_N}) in terms of the significant geophysical and meteorological conditions. In general, the meteorological conditions include mean wind speed and atmospheric stability in relation to topography, height, time of day, and seasonal parameters. In the previous studies (refs 1-4), it was concluded that the interdependence of some of these conditions was sufficiently weak to permit a relatively straightforward application of Equation (1). A summary of these conditions is as follows:

1) The form of the normalized vertical gust spectrum (φ_{w_N}) is considered independent of atmospheric stability when the frequencies are divided by the true airspeed; the spectrum form depends only on the height above the surface and the terrain roughness (see refs 1 and 2).

2) Over smooth terrains, the rms turbulence intensity (σ_w) is considered to be principally related to mean wind speed and parametrically related to atmospheric stability. Over rough terrains the rms gust velocities are considered independent of stability (refs 3 and 4).

3) The probability distributions of the climatological wind speeds are considered independent of height and atmospheric stability, and weakly dependent on terrain conditions, when the mean wind distributions are normalized by the appropriate average mean wind speeds representing height and stability classifications (see refs 3 and 4). This wind speed behavior enables the $f(\sigma_w)$ function to be specified on the basis of the rms turbulence intensity function and the average mean wind speed.

In Section 6 of this report, the average mean wind or climatic wind speed (as it is referred to in refs 2-4) characteristics are considered for representative locations in the United States. These wind data are summarized for both smooth and rough terrain conditions for such factors as atmospheric stability and height above the surface for diurnal, seasonal, and yearly periods.

Section 3

SPECTRUM SHAPE

The form of the normalized spectrum function is described in refs 3 and 4 for the low-level regime. The spectrum function representation is based on the B66 data, as well as a number of aircraft and tower measurements. Tower measurements have been used because they may provide an indication of the behavior of the longer wavelength spectral components, as shown in Figure 1.

The spectrum function presented in Figure 1 is of the form

$$\varphi(k) = 2\pi L/(1 + 2\pi kL)^2 \tag{3}$$

where $k = f/U$ is a wave number (reciprocal wavelength), f is the frequency in cycles/sec, U is the true airspeed in ft/sec, and L is a scale parameter in feet related to the terrain roughness and height above the ground.

Although Equation (3) does not provide for a -5/3 power law behavior at the smaller wavelength (about 100 ft), Figure 1 indicates the relatively small differences that exist between the spectrum estimates for a -5/3 and a -2 power law. Since it is difficult to conclusively prove the existence of either of these power laws from present measurements, Equation (3) is considered a reasonable representation for the spectrum form in the low-level regime.

The scale parameter L for the B-66 data was estimated for four terrain and three height (200, 600, and 1000 ft) classifications as shown in Figure 1 of refs 3 and 4. In view of the relatively small differences observed in the smooth terrain farmlands and woodlands classifications (both with respect to L and subsequent wind speed characteristics), a single smooth terrain scale parameter is believed adequate. The linear scale parameter with height relationship is

$$L = h_o + h\,L_h \quad . \tag{4}$$

The values of L_h and h_o for each terrain are shown in Table 1. In Equation (4), L is assumed constant above 1000 ft.

Table 1. Values of L_h and h_o for each terrain.

Terrain Class	L_h	h_o
Smooth	2/3	135
Low Mountains	1/2	300
High Mountains	1/8	675

Section 4

VERTICAL VELOCITY RMS BEHAVIOR WITH MEAN WIND SPEED

1. Smooth terrain estimates

Smooth terrain vertical velocity rms estimates as a function of mean wind speed, based on the B-66 data, are presented in refs 3 and 4 for three atmospheric stability classifiçations. Although the B-66 wind and stability estimates were not considered highly reliable, the rms functions obtained from the data were found to be in reasonable agreement with meteorological tower data.

In the analysis of the climatic-wind-speed data conducted in the present study, only a relatively few (about 15 percent) neutral stability cases (see Section 6) were encountered. This suggests a possible simplification to the model procedure by including the neutral cases in the unstable classification. Under this simplification, relations for the rms gust velocity as a function of mean wind speed would be represented by

$$\sigma_w = 0.1\ u \tag{5}$$

and

$$\sigma_w = 1.65 + .08\ u \tag{6}$$

for stable and unstable conditions, respectively; where u is the mean wind speed in ft/sec. In accordance with ref 3, the σ_w functions are considered to be independent of height.

Although the stable expression (5) is believed to be reasonable for low-to-moderate wind speed conditions, it does not appear reasonable to have the stable σ values exceed the unstable σ values for large wind speed

conditions. For this reason, and because only the high wind speed conditions are generally of interest in aircraft gust load problems, it is proposed to use the unstable expression to represent the rms-mean-wind-speed behavior in the present gust load model.

In the application of Equation (6) the regression constants should be increased to allow for statistical variability in σ_w as discussed in refs 3 and 4. Based on 95% confidence limits for the σ_w data used to obtain the regression equation, Equation (6) becomes

$$\sigma_w = 2.45 + .12\,\bar{u} \tag{7}$$

or, in terms of m/s,

$$\sigma_w = .75 + .12\,\bar{u} \tag{8}$$

2. Rough terrain estimates

As described in ref 3, the effect of atmospheric stability could not be separated from the scatter of the rough terrain σ_w estimates. The least squares linear regression lines for the low and high mountains σ_w estimates reported in refs 3 and 4 were noted to be approximately equal for both rough terrain categories. The principal difference between the two sets of data being the much greater scatter observed for the high mountain σ_w estimates.

In view of the closeness of the two regression functions, it is suggested that a single expression be used for both rough terrain categories; namely,

$$\sigma_w = 3 + .05\, u \tag{9}$$

where u is in ft/sec. However, because of the difference in the statistical variability of the estimates, the equations used in the gust load model are different. Thus, for 95% confidence limits, the function for the low mountain case is

$$\sigma_w = 1.3 + .07\, \bar{u}; \tag{10}$$

whereas, the equivalent expression for the high mountain terrain classification is

$$\sigma_w = 1.8 + 0.1\, \bar{u} \tag{11}$$

where $\bar{u}$ is expressed in m/s.

Section 5

CLIMATOLOGICAL WIND SPEED DISTRIBUTIONS

1. Previous data

A description of the mean wind speed distribution characteristics for smooth and rough terrain conditions is presented in refs 2-4. The smooth terrain distribution characteristics obtained in ref 2 are based on radiosonde and pibal observations obtained at Dayton, Ohio from June 1956 to May 1958. For these data the following factors were considered: atmospheric stability, seasons, time of day, and height.

The results of additional climatological data analyses for both smooth and rough terrain locations were reported in refs 3 and 4. For these results the smooth terrain data used were for June 1953 through May 1957, for 1000 and 1600 EST at Dayton and for 1500 CST at Fort Worth, Texas. The rough terrain data were for Medford, Oregon, Las Vegas, Winnemucca, and Ely, Nevada and Boise, Idaho for 1200 and 2400 GMT. The height range for the rough terrain data extended from the surface to 5000 m above the surface.

2. Present data

To provide a more extensive climatic and geographical coverage for the climatological wind data, the data summarized in Table 2 were obtained from the National Weather Records Center (ESSA), Asheville, North Carolina:

Table 2. Climatological data summary

STATION	PERIOD OF RECORD	TIME (LST)	HEIGHT RANGE (above surface, meters)
San Diego, Cal.	1958-1959	1600(PST)	0-3000
El Paso, Tex.	1958-1959	1700(MST)	0-5000
Denver, Colo.	1958-1959	1700(MST)	0-6000
Oakland, Cal.	1958-1959	1600(MST)	0-3000
Bismark, N. Dak.	1958-1959	1700(MST)	0-4000
Lander, Wyo.	1958-1959	1700(MST)	0-6000
Seattle, Wash.	1958-1959	1600(PST)	0-3000
Gt. Falls, Mont.	1959-1959	1700(MST)	0-5000
Tucson, Ariz.	1960-1961	1700(MST)	0-4000
Sault St. Marie, Mich.	1955-1956	0900(CST)	0-762
Topeka, Kans.	1955-1956	0900(CST) 1500(CST)	0-762
Montgomery, Ala.	1955-1956	0900(CST) 1500(CST)	0-762
Norfolk, Va.	1955-1956	1000(EST) 1600(EST)	0-762

3. Wind distributions

As described in ref 3, a general wind probability density distribution was obtained for the four conditions listed above by using dimensionless wind speed $(u/\bar{u})$ as the independent variable, where $\bar{u}$ is the average mean wind speed associated with a particular condition, e.g., height above the surface, referred to as "climatic-wind-speed".

In ref 3, a small difference in the form of the dimensionless wind speed density distribution was noted for the smooth and rough terrains. The present data indicates a third variation in the probability density form; Figure 2 summarizes the three distribution forms. For the present data,

all rough terrain stations exhibit greater probability density values at large $u/\bar{u}$ values than the previous rough terrain stations. In addition, the Norfolk and Montgomery data also conform to this third distributional form.

The nearest analytic representation found for the density distributions is of the form described in ref 2:

$$p(x) = G_1 G_2 \, x^{G_2 - 1} \, e^{-G_1 x^{G_2}}$$

where $x = u/\bar{u}$; G_1 and G_2 are arbitrary parameters. This distributional form was first used by Weibull (ref 6) to describe the observed behavior of many physical random variables. Suggested values of G_1 and G_2 to approximate the wind distribution behavior are presented in Figure 2. It appears difficult, however, to obtain a close approximation to the observed data with this representation.

Section 6

CLIMATIC MEAN WIND SPEED CHARACTERISTICS

1. Wind data

To use the climatological wind speed distributions described in Section 5, a systematic means of specifying climatic mean wind speed values ($\bar{u}$) is necessary for the continental United States. To examine surface and upper level wind speed data for this purpose, the NWRC data presented below were obtained for the surface and for heights ranging up to 6000 m above the mean sea level (MSL). The data were obtained as monthly averages of hourly data at the surface, and for 1800 and 2400 GMT for the upper levels.

A summary of the climatic-wind-speed data, averaged for the years listed in Table 2, is presented in Table 3. Small year-to-year variations (less than 10 percent) were observed in the wind speed averages.

2. Rough terrain

(a) Height variation - In considering the height profiles of the climatic wind speeds, the $\bar{u}$ values of Table 3 were averaged for the two hourly periods shown, since the differences in the $\bar{u}$ values for the two periods are quite small at the upper levels.

In ref 3, the rough terrain $\bar{u}$ values were divided by the $\bar{u}$ surface values in an effort to generalize the wind speed behavior with height. Based on the additional data analyzed in the present study, this procedure appears less desirable because of the variability observed in the surface $\bar{u}$ values. Figures 3 and 4 show the $\bar{u}$ values for 14 rough terrain stations and 4 smooth terrain stations. It is observed that the variations from the

Table 3. Climatic-wind-speed summary.

Station	(LST)	sfc	Height(m) 1000	2000	3000	4000	5000	6000
New York	1900	5.7	10.2	12.1	14.6	17.3	20.2	23.2
(N. Y.)	1300	6.1	9.5	12.4	14.2	17.9	20.6	23.7
Dayton	1900	4.5	9.7	11.0	13.3	16.0	18.4	21.0
(Ohio)	1300	5.3	10.1	10.5	12.8	15.2	17.7	20.3
Montgomery	1800	3.3	7.0	8.8	10.0	13.2	15.2	17.6
(Alabama)	1200	4.2	7.0	9.4	11.0	13.0	14.8	17.4
Topeka	1800	6.3	9.2	10.7	12.6	14.7	16.8	18.8
(Kansas)	1200	6.5	9.0	11.2	12.8	14.5	16.6	18.6
Great Falls	1700	6.4	8.9	10.8	13.6	16.4	18.8	—
(Montana)	1100	6.1	8.8	10.7	13.2	15.8	16.5	—
Long Beach	1600	4.8	—	—	—	—	—	—
(California)	1000	2.4	—	—	—	—	—	—
Santa Monica	1600	—	4.1	5.9	8.7	10.8	12.7	14.7
(California)	1000	—	4.0	6.3	8.8	11.0	12.6	14.6
Oakland	1600	5.7	5.8	7.2	9.0	—	—	—

Station	(LST)	sfc	900	1400	2400	3400	4600
Denver	1700	4.8	6.2	6.8	9.5	13.0	15.8
(Colorado)	1100	3.8	5.7	6.9	9.9	13.0	15.4

Station	(LST)	sfc	900	1300	1800	2200	3800
El Paso (N. Mexico)	1700	5.8	6.0	6.8	7.9	10.2	11.8

Station	(LST)	sfc	1000	1500	2000	2500	3500
Bismarck (N. Dakota)	1700	6.5	8.8	9.1	10.3	11.7	13.8

Station	(LST)	sfc	800	1300	2300	3300	4300
Lander (Wyoming)	1700	3.8	5.2	6.4	10.1	13.2	15.8

Station	(LST)	sfc	700	1200	1700	2200	3200
Tucson (Arizona)	1700	5.2	5.7	5.9	6.4	7.1	9.7

All wind speeds in m/s.

average profiles shown are less than ± 20 percent, and that the standard error of estimate for the rough terrain data is about one (1) m/s.

Of the 14 rough terrain stations analyzed, only the West Coast Santa Monica and San Diego profiles characteristically depart from the average, suggesting that the $\bar{u}$ profiles, in general, do not depend on geographical location. It is interesting to note that the rough terrain and smooth terrain profiles converge at the higher elevations, as shown in Figure 5. It would appear that the obstructing effect of mountainous terrain produces a steeper wind profile for the first 1500 meters, or so, above the surface, and that orographic effect gradually diminishes with height and then disappears at about the 3000 to 4000 meter level.

(b) Seasonal variations - To determine the seasonal variation, the monthly averages for six of the stations* of Table 2 were divided by the corresponding "period of record" averages listed in Table 3, and this dimensionless value was plotted for each month and for each elevation above the surface from 1000 to 5000 meters. Since differences between the forenoon and afternoon values were minor, the two daily readings were combined for each of the six stations and the monthly-to-yearly wind speed ratios $(\bar{u}_m/\bar{u}_{an})$ plotted for each height. The results for the 2000 m elevation are shown in Figure 6. The scatter about the mean of the $\bar{u}_m/\bar{u}_{an}$ values for the 2000 m level is similar to the scatter observed for the four other elevations. The mean values for all five elevations are shown in

*The Denver station elevation of 1600 m(MSL) precluded conveniently including this station in the even numbered height-above-station classification.

Figure 8, where the four single year distributions are shown for the New York station (1961 to 1964) for the 2000 m level.

3. Smooth terrain

(a) Seasonal variation - The monthly variations of the $\bar{u}_m/\bar{u}_{an}$ wind speed ratios at the surface are shown in Figure 9 for the four smooth terrain stations. The year-to-year variations for the New York station are shown in Figure 10. Although the year-to-year single station variations at the surface are seen to be greater than the upper level year-to-year distribution (Figure 8), the station-to-station variability of the averaged $\bar{u}_m/\bar{u}_{an}$ values of Figure 9 are comparable to those of Figure 6 for the upper levels. The principal difference between the surface and upper level distributions is the greater skewness of the surface distribution. The seasonal variation of the wind speeds at the 300 m level are described under (c) below.

(b) Diurnal variation - Surface wind speeds obtained from hourly data are shown in Figures 11 and 12 for four smooth terrain stations and Long Beach. These figures indicate that the year-to-year variations for all stations are comparatively small. In Figure 13 the envelope of the monthly averages are shown for Dayton for 1961.

To generalize the diurnal wind speed behavior, the average hourly distributions of Figures 11 and 12 were divided by the 1500 local standard time wind speeds, which represent the approximate daily maximum values. The results of this normalization, shown in Figure 14, reveals a fairly consistent pattern of diurnal variations from about 0800 to 1700 (LST), although both the early morning and evening wind speed averages are seen to differ by as much as 10% from the mean at particular stations.

The drastic change in the behavior of the Long Beach surface winds is believed to be produced by the proximity of the ocean and the California current off the coast of southern California. The over-water trajectories of the westerly winds provide relatively small wind speeds through most of the day; however, the development of an afternoon sea breeze in this region may be the reason for the increase in the mean wind speed values during the mid-afternoon period, raising the wind speed values to about the average of the other continental stations. In Table 4 the 1500(LST) average wind speeds are listed for both rough and smooth terrain stations; the average for the smooth terrain stations is just under 5.5 m/s, while the rough terrain station average is 6 m/s. The Long Beach-San Diego average is 5 m/s. As a matter of interest, it was ascertained that the diurnal surface wind variations for the rough terrain stations were substantially similar to the smooth terrain variations.

(c) Atmospheric stability conditions - In ref 2, the effect of atmospheric stability on the mean wind speed values was examined in considerable detail for two smooth terrain locations: Dayton, Ohio and Fort Worth, Texas. In the present study, stability wind speed data for three additional smooth terrain stations were obtained. The stability criteria used for these data was the temperature difference between the 300 m level and surface station. A temperature difference less than 5°F was considered stable, between 5°F and 6°F neutral, and greater than 6°F unstable. Soundings were available for both morning and afternoon at the three stations. A summary of the frequency of occurrence, mean wind speed, and stability distribution (in percent) for each sounding period is summarized in Table 5

Table 4. Summary of climatic-wind-speed values at the surface for 1500 LST.

Station	Wind Speed (m/s)	Station	Wind Speed (m/s)
Dayton (Ohio)	5.5	El Paso (Texas)	6.2
Norfolk (Virginia)	5.2	Tucson (Arizona)	5.7
Topeka (Kansas)	6.3	Lander (Wyoming)	4.9
Montgomery (Alabama)	4.4	Great Falls (Montana)	7.0
New York (New York)	6.3	Denver (Colorado)	5.0
Long Beach (California)	4.8	Bismarck (N. Dakota)	7.0
San Diego (California)	5.2	Oakland (California)	6.2
Sault St. Marie (Michigan)	5.1	Seattle (Washington)	5.8

Table 5. Smooth terrain climatic-wind-speed ratios for three stability conditions.

		$\bar{u}_{300}/\bar{u}_{sfc}$			Frequency (percent)			$\bar{u}_{sfc}$		
Station	(LST)	S	N	U	S	N	U	S	N	U
Dayton	0930	2.1	1.7	1.7	69	11	20	3.5	4.4	3.7
(Ohio)	1530	1.8	1.5	1.5	38	26	36	4.5	3.8	4.2
Norfolk	1000	1.6	1.5	1.5	65	10	25	5.1	5.5	5.8
(Va.)	1600	1.6	1.4	1.3	57	16	26	5.3	5.4	5.0
Montg.	0900	2.1	1.7	1.5	50	12	38	3.2	3.7	3.2
(Ala.)	1500	1.8	1.4	1.5	29	17	54	4.2	4.3	3.6
Topeka	0900	1.6	1.5	1.4	73	8	19	5.1	5.0	5.5
(Kans.)	1500	1.3	1.2	1.2	30	22	48	6.1	6.7	6.3

for the five smooth terrain stations. In addition, Table 5 presents 300 m-to-surface wind speed ratios for each stability condition.

In Table 5, the wind speed ratios($\bar{u}_{300}/\bar{u}_{sfc}$) for the neutral and unstable conditions are seen to vary much less than the same wind speed ratios for the stable classification. Moreover, if the wind speed ratio is plotted with the surface wind speed, as in Figure 17, the stable ratios are shown to decrease with increasing $\bar{u}_{sfc}$ values. The wind speed ratios for both the neutral and unstable conditions, on the other hand, do not correlate as well with the $\bar{u}_{sfc}$ values. In fact, below about 6 m/s the neutral and unstable ratios vary only about 10 percent from a mean value of about 1.5.

The relatively small number of neutral stability cases indicated by the data of Table 5, and the small difference in the $\bar{u}_{300}/\bar{u}_{sfc}$ ratios for the neutral and unstable cases, suggest the possibility of combining these two stability classes into one grouping for modeling purposes. On this basis, the diurnal distribution of the relative number of unstable (neutral and unstable combined) cases are shown in Figure 18 as a function of local standard time. Although these results do indicate variations from station to station, no specific geographical trend is discernible. The approximate behavior indicated in the figure is suggested to represent the relative occurrence of unstable stability conditions between the hours of 0600 and 1800 LST.

The wind speed ratio values in Figure 17 (stable cases only) can be approximated by the expression

$$\frac{\bar{u}_{300}}{\bar{u}_{sfc}} = 2.9 - .26\,\bar{u}_{sfc} \qquad (12)$$

For intermediate altitudes of 150 and 60 meters, the profile characteristics reported in refs 2 and 3 are used to approximate $\bar{u}_{150}/\bar{u}_{sfc}$ and $\bar{u}_{60}/\bar{u}_{sfc}$ ratios. Using Figure 15 of ref 2, and the data of Figure 17, the wind speed ratios for the stable condition at 150 and 60 meters are represented by

$$\frac{\bar{u}_{150}}{\bar{u}_{sfc}} = 2.3 - .18\,\bar{u}_{sfc} \,. \tag{13}$$

and

$$\frac{\bar{u}_{60}}{\bar{u}_{sfc}} = 1.8 - .10\,\bar{u}_{sfc} \,. \tag{14}$$

Under neutral to unstable stability conditions the average wind speeds do not vary appreciably between the 500 ft (150 m) and 1000 ft (300 m) levels, as shown by Figure 17 of ref 2. At 150 m the $\bar{u}_{150}/\bar{u}_{sfc}$ ratio from ref 2 is about 1.5, in approximate agreement with the data of Table 5. Hence, these values are used in the present model.

The seasonal variation of the climatic-wind-speeds at 300 m for stable and unstable conditions were considered for the available morning and afternoon time periods of 1500 and 2100 GMT. For the stable data, the monthly-to-yearly wind ratios did not vary significantly for the two time periods; however, the seasonal distributions for the unstable data are shown in Figure 16 to be decidedly dissimilar for the two time periods. The wind speed ratios for the stable condition are shown in Figure 15. The smooth curves in these figures are suggested representions for the three set of data.

Section 7

GENERALIZED LOAD EXCEEDANCE CURVES

Based on the results of Sections 4-6, generalized load exceedance design curves can be obtained from Equation (1). For this purpose, Equation (1) is expressed as

$$\frac{N(Y)}{N_o} = \int_0^\infty f(\sigma_w) \exp\left\{-\frac{\chi^2}{2\sigma_w^2}\right\} d\sigma_w \tag{15}$$

where $\chi = Y/A$.

For specified values of χ, Equation (15) is evaluated for an average probability density function of mean wind speed (Figure 2) and a range of values of α, b, and $\bar{u}$, representing the σ_w dependence on mean wind speed:

$$\sigma_w = \alpha + b\,\bar{u}$$

The α and b values were described in Section 4 for the smooth and rough terrain conditions; the characteristics of $\bar{u}$ were described in Section 6. Since both b and $\bar{u}$ vary, the product $b\bar{u}$ is represented by β below.

Solutions for Equation (15) were obtained for four specific values of χ: 7, 14, 21, and 28. These solutions were obtained for β values ranging from 0.5 to 1.8 for parametric values of α of 0, 0.5, 1.0, 1.5, and 2.0. These solutions are shown in Figure 20.

To obtain solutions for values of χ and α intermediate to those shown in Figure 20, cross-plots can be constructed. For instance, to

evaluate intermediate values of α (for a given χ). N/N_o values are plotted as a function of α for a given value of β; intermediate values of α are then obtained from the curve drawn through the five α values provided by Figure 20. Similarly, intermediate values of Y/A can be obtained from a plot of N/N_o versus χ for given values of α and β.

Section 8

MODEL PROCEDURES

In Sections 3 and 4, the spectrum shape function and vertical velocity rms characteristics with respect to terrain roughness were described. In Sections 5 and 6 (and refs 2 and 3), the climatological wind speed probability distributions and climatic-wind-speed characteristics with respect to such variables as height, seasons, atmospheric stability, time of day, and terrain roughness were presented. In Section 7, generalized load exceedance curves were presented to permit relatively easy evaluation of N/N_o as a function of Y/A for the parameters (α, β) representing the σ_w dependence on terrain, height and climatic-wind-speed conditions. In this section, an outline of procedures is presented for utilizing detailed climatological wind speed characteristics for estimating gust load exceedance probabilities. Also, an illustration of the application of these procedures is presented for the rough terrain case.

1. Smooth terrain procedure

The average number of peak values per unit distance exceeding a given load level is given by Equation (15). For a given height above the surface and a given true airspeed, A^2 and N_o depend on the normalized spectrum function and the aircraft dynamic response function $T(i\Omega)$. For a particular height and aircraft flight condition (true airspeed, weight, etc), the procedure for evaluating Equation (15) for smooth terrain conditions is described below, and in flow chart form in Figure 21. For the present it is assumed that all smooth terrain conditions are sufficiently similar to

permit using the statistical averages obtained from the present study. It is possible, however, that for some applications it may be desirable to evaluate the model for specified smooth terrain locations.

1) The "operational day" is divided into a number of "diurnal time units", disregarding, for the present, the relative amount of time spend in each unit. Selection of time units or blocks is based on Figure 14.

2) The daytime maximum surface climatic-wind-speed value for a specific smooth terrain location is selected (see Table 4), or a value of 5.5 m/s is used to represent general smooth terrain conditions. Wind speed values corresponding to diurnal time units of step (1) are obtained from Figure 14.

3) Select "seasonal blocks" on the basis of Figures 15 and 16 to represent seasonal changes in climatic-wind-speed. For each stability condition multiply the wind estimates of step (2) by the appropriate values from Figures 15 and 16. (The monthly changes in the wind speeds at 300 m, represented by these figures for stable and unstable conditions, are also used to represent the changes at the 150 and 60 meter levels).

4) For stable atmospheric stability conditions, the climatic-wind-speed values at a given flight level are obtained from the surface values of step (3) and one of the Equations (12-14) based on Figure 17. For unstable stability conditions, the flight level climatic-wind-speeds are obtained by increasing the surface wind speeds by 50 percent for the 300 m and 150 m levels, and by 35 percent for the 60 m level, in accordance with Section 6.

5) Using the $\bar{u}$ values of step (4) and the vertical velocity rms function [Equation (7) and (8)], estimate α and β for the stable and unstable conditions.

6) For selected Y/A values, determine N/N_o for α and β [step (5)] from Figure 20.

7) Figure 18 is used to divide each diurnal time unit of step (1) into a stable portion; and a relative exposure weight (REW) is assigned to represent the percent of smooth terrain flight time at each diurnal time unit for each location, height, and season.

8) Using the numerical weights determined in step (7), N/N_o values are determined for stable and unstable conditions. (N_1;N_2 in Figure 21).

9) Add the N/N_o values of step (8): $(N_1 + N_2)/N_o = N_i/N_o$.

10) Repeat steps (1) through (9) for each time and seasonal unit selected (for a given height and location):

$$\frac{1}{N_o} \sum_{ij} N_{ij}(Y) = \frac{1}{N_o} N_{zk}(Y)$$

where i and j represent time and seasonal units and z and k height and location.

11) Repeat steps (1) through (10) for each location desired. Thus,

$$N/N_o(Y) = \frac{1}{N_o} \sum_{k} N_{zk}(Y) = \frac{1}{N_o} N_z(Y)$$

where $N_z(Y)$ represents the summation over j and k for a single height z.

12) Evaluate N_o for height above surface used in steps (1) through (11).

13) Repeat steps (1) through (11) for each additional height desired. Sum the N(Y) results for all heights selected:

$$N(Y)_{\text{Smooth terrain}} = \sum_{z} N_z(Y) \ .$$

2. Rough terrain procedure

The procedure followed for the rough terrain cases is similar to the smooth terrain, except that neither atmospheric stability nor diurnal variations of the upper level wind speeds need be considered. For a particular height and aircraft flight condition the rough terrain procedure is described below and in flow chart form in Figure 22. As in the smooth terrain case, the climatic-wind-speed statistics are not related to particular locations; although, as for smooth terrains, it is possible to consider particular terrain locations, when necessary.

1) Apportion flight time over rough terrain between low and high mountain conditions; and determine the average flight levels (above the surface stations) for the terrain locations selected. (See discussion below).

2) Use Figure 3 to estimate climatic-wind-speeds for the heights selected in step (1).

3) Use Figure 7 to adjust the wind speed values obtained from step (2) for seasonal variations.

4) Using the $\bar{u}$ values of step (3) and the rough terrain rms functions [Equation (10) and (11)], estimate α and β for each function.

5) Determine values of A for heights z_i selected for high and low mountain.

6) For values of A of step (5) and a selected Y, determine N/N_o for α β of step (4) from Figure 20.

7) Assign relative exposure weights for each height to represent percent of rough terrain flight time at height z_i above the surface. Designate this ζ_i. Also assign a relative weight for the percent of rough terrain flight time over high mountain terrain. Designate this r; $(1 - r)$ is then the percent of rough terrain flight time over low mountain terrains.

8) Using the relative weights of step (7), the low mountain and high mountain N/N_o values are obtained (N_3/N_o and N_4/N_o in Figure 22).

9) Evaluate N_o for the heights selected for the low and high mountain (z_i).

10) Multiply results of step (8) by the N_o values of step (9).

11) Add the load exceedance probabilities N_3 and N_4 for the low and high mountain cases.

12) Repeat steps (1) through (11) for each additional height and seasonal block desired.

$$N_k = \sum_{zj} N_{zj}(Y)$$

13) Repeat steps (1) through (12) for specific locations desired.

$$N(Y)_{\text{Rough terrain}} = \sum_{k} N_k(Y)$$

Finally, to combine the load exceedance estimates $N(Y)_{\text{Smooth}}$ and $N(Y)_{\text{Rough}}$, it is necessary to provide relative weights for flight time divided between smooth and rough terrains. Thus,

$$N(Y) = n\,N(Y)_{\text{Smooth}} + (1 - n)\,N(Y)_{\text{Rough}}$$

where n is the percent flight time over smooth terrains.

3. Illustration of application of model

As an illustration of detailed application of the gust load model summarized in Figures 21 and 22, the following rough terrain conditions will be assumed:

z_1 (low mount) = 1000 m

z_2 (high mount) = 3000 m

m (seasonal unit) = January

Y/A (exceedance value desired) = 14

ζ_i (percent flight time at z): $\zeta_1 = .4$; $\zeta_2 = .2$

r (percent flight time over high mountains) = .4

N_o (characteristic frequency) = .5

Using the above data and the flow chart of Figure 22, the solution for $N_3(Y)$ and $N_4(Y)$ are easily obtained. The steps performed for this solution are indicated in Figure 23, where the steps indicated in Figure 22 have been evaluated in accordance with the assumed data above.

4. Rough terrain classification

To determine the height above the surface to use in the model it is necessary to consider flight path profiles in relation to rough terrain profiles. For this task some criteria to describe the difference between the low and high mountain terrain classification is necessary. Inasmuch as this terrain differentiation was originally used in the B-66 program, the rough terrain track profiles reported by Douglas are shown in Figure 12.

In examining these profiles, in conjunction with rms vertical velocity data, it appears that the low mountain (less roughness) classification might include profiles 21 and 22 at Kirtland as limiting profiles for the low mountain category; tracks 11 and 12 at Kirtland and 11 at Edwards appear

to be very nearly equal in roughness to 21 and 22 for Kirtland. The remaining high mountain profiles (21 Edwards and Shaw, 23 Edwards and Kirtland, and 24 Edwards) provide considerably greater scatter in the rms gust velocity data. Based on these rough terrain profiles it is suggested that the low mountain terrain classification include terrain profiles whose peak-to-valley differences (over 20 to 30 mile segments) lie between 500 to 2000 ft; and that the high mountain classification include all profiles with peak-to-valley differences exceeding 2000 ft.

For estimating rough terrain topographical profiles, two series of USAF Navigational Charts are available. These are (1) USAF Jet Navigation Charts, and (2) USAF Operational Navigation Charts. They are available from the Department of the Air Force, Headquarters, Aeronautical Chart and Information Center, Second and Arsenal, St. Louis, Missouri 63118.

Section 9

PRELIMINARY COMPARISON WITH B-52 DATA

As a preliminary comparison of the turbulence model with available aircraft data, load history exceedance values reported by Boeing for the B-52 aircraft were considered.

Although it was not possible in the present program to conduct a detailed comparison of the Boeing load data with the turbulence model, rough comparisons were made based on $N(Y)/N_0$ versus Y/A summaries presented in refs 9-11.

Before discussing the results of this comparison, some of the problems associated with the B-52 data for the G/H and B-F aircraft are described. For present purposes there are two principal limitations that reduce the usefulness of the B-52 data as a test for the turbulence model:

1) The oil burner routes were flown at a minimum terrain-clearance altitude of 800 ft over the plains, and several thousand feet over the mountains. The poker deck routes were flown down to 500 ft terrain clearance. The poker deck data, however, represents only about 7 percent of the total low-level experience and detailed summaries of these flights are not available.

2) The B-52 was operating under flight restrictions which precluded recording some of the more severe gust load data.

Keeping these facts in mind, summaries of $N(Y)/N_0$ versus Y/A were obtained from ref 9-11. The summaries are shown in Figure 24. The following is observed about the B-52 data: 1) The average terrain-clear-

ance height for the low-level data is about 2500 ft; 2) For the available 800 ft data, the 800 ft poker deck exceedances are slightly greater than the 800 ft oil burner exceedances - apparently reflecting the influence of contour flying in the poker deck data; 3) The 800 ft exceedances are considerably greater than the 2500 ft data, indicating the influence of the earth's surface on the turbulence intensities; 4) The relatively high terrain-clearance altitude flown for the oil burner routes appears to have washed out the terrain influence, as shown by the very close agreement between the Plains and Mountains data report in ref 11.

In order to obtain a rough comparison at this time of the NYU model with the B-52 data no attempt was made to take into account detailed flight conditions. Instead, it is assumed that on the basis of the $\bar{u}$ climatic wind speed behavior described in Section 6 an average $\bar{u}$ value between 7 and 8 m/s can be taken as representative of wind speed conditions encountered in the B-52 program for the 800 ft data. Note that the Y/A values for the model are in m/s and must be multiplied by 3.28 to correspond to Y/A of the measured load data. The model $N(Y)/N_o$ estimates for Y/A values of 23 and 46 are indicated in Figure 24 for an assumed smooth terrain $\bar{u}$ value of 7.5 m/s at an altitude of 800 ft above the surface.

Section 10

DISCUSSION OF MODEL APPLICATION

An outline of procedures for applying the low altitude turbulence model to estimate aircraft gust loads was presented in Section 8. The actual experience of using the model will determine the necessity of modifying or simplifying the steps outlined. A very rough comparison of the model was made in Section 9 with a limited amount of B-52 load exceedance data obtained over smooth terrain at an approximate terrain-clearance altitude of 800 ft. In general, two kinds of "model experience" exercises should be considered.

First, the sensitivity of the model should be tested to evaluate the effect of (1) modifying the climatic-wind-speed probability density function for smooth terrain and rough terrain conditions,and (2) changing the number of incremental divisions used to represent the physical conditions of height and diurnal/seasonal blocks.

Second, the operational histories of low-altitude gust load programs, such as the B-52 flight loads program, should be used as input data to the turbulence model to provide such details as airspeeds, aircraft weights, terrain-clearance altitudes, track locations, time of day and season. The predicted model results can then be compared directly with the measured service load data. Such comparisons would serve also to provide statistical criteria for the confidence limits required to describe the rms gust velocity as a function of mean wind speed.

Section 11

SUMMARY AND RECOMMENDATIONS

In the present study the following results were obtained in the development of a low-level turbulence model:

(1) Probability density distribution functions of mean wind speed to climatic mean wind speed ($u/\bar{u}$) were determined for smooth and rough terrain conditions.

(2) Climatic mean wind speed variations with height were described for smooth and rough terrain conditions.

(3) Monthly variations of the climatic mean wind speed ratios ($\bar{u}_m/\bar{u}_{an}$) were obtained for smooth and rough terrain conditions. For smooth terrains, the monthly variations were obtained for the surface and 300 meter levels. For rough terrains, the upper level wind speed ratios were found essentially independent of height.

(4) The diurnal variation in the relative number (percent) of unstable atmospheric stability conditions occurring for smooth terrain stations was estimated. In this estimate the neutral conditions were included in the unstable classification, since only about 15 percent of the cases (on the average) were found in the neutral category.

(5) For smooth terrain conditions, the daytime variations in the climatic mean wind speeds were described and a representative function ($\bar{u}_H/\bar{u}_{max}$) was obtained. The maximum climatic mean wind speed values were found to occur at about 1500 LST.

(6) Based on the climatic mean wind speed characteristics obtained in the study, procedures were outlined for applying the low-level turbulence model to gust load exceedance estimates.

(7) A rough comparison of the gust load exceedance values obtained by B-52 aircraft operating at approximate 800 ft terrain-clearance heights over plains and the turbulence model values for smooth terrain conditions was made.

On the basis of the low-level model developed, the following recommendations are made:

(1) The sensitivity of the model should be tested to determine (a) the number of incremental steps (or blocks) required to adequately define the environmental conditions (e.g. height; diurnal and seasonal variations) and (b) the effect of using separate probability wind speed density functions to represent smooth and rough terrain conditions.

(2) The model predictions should be compared with available low-altitude load exceedance data. For such comparisons the environmental conditions of time of day and year, and topography associated with measured data should be available.

(3) Additional aircraft measurements of rms gust velocity and associated wind speed should be obtained to more adequately establish the relationship between the two quantities.

REFERENCES

1. Lappe, U. O. and J. Clodman. On Developing a Low Altitude Turbulence Model for Aircraft Gust Loads. ASD-TDR-62-152. Aeronautical Systems Division of the Air Force Systems Command, Wright-Patterson AFB, Ohio, March 1962.

2. Lappe, U. O., R. H. Thuillier, and R. W. Reeves. Development of a Low Altitude Turbulence Model for Estimating Gust Loads on Aircraft, ASD-TDR-63-318. Aeronautical Systems Division of the Air Force Systems Command, Wright-Patterson AFB, Ohio, July 1963.

3. Lappe, U. O. Design of a Low Altitude Turbulence Model for Estimating Gust Loads on Aircraft, AFFDL-TR-64-170. Air Force Flight Dynamics Laboratory, Research and Technology Division of the Air Force Systems Command, Wright-Patterson AFB, Ohio, March 1965.

4. Lappe, U. U. "Low Altitude Turbulence Model for Estimating Gust Loads in Aircraft". AIAA Jour. of Aircraft, Vol. 3, No. 1, January-February 1966.

5. B-66B Low Level Gust Study. WADD TR 60-305, Wright Air Development Division, Wright-Patterson AFB, Ohio, March 1961. 14 Vols.

6. Weibull, W. "A Statistical Distribution Function of Wide Applicability". Jour. Appl. Mech. 18: 293, 1951.

7. Kirwan, A. D., Jr., S. L. Adelfang, and G. J. McNally. Laboratory and Field Evaluation of Thrust Anemometer. N. Y. U. Final Report under NSF Grant No. 3850, December 1966.

8. Gurvich, A.S. "Frequency Spectra and Functions of Probabilities Distributions of Vertical Wind Velocity Components". Izv. Akad. Nauk SSSR, Ser. Geofiz 7, 695-703, 1960.

9. An Analysis of the Correlation Between Turbulence Encountered During B-52 G/H Low Level Operations and Synoptic Meteorological Data. Boeing Document No. D3-6649, 1965.

10. Yost, J. D. Flight Loads Data Collection Programs. OCNEA Structures Note 65-2. Tinker AFB, Oklahoma.

11. Final Summary of B-52 G/H Flight Load History Program. Boeing Document No. D3-6497. 31 August 1964.

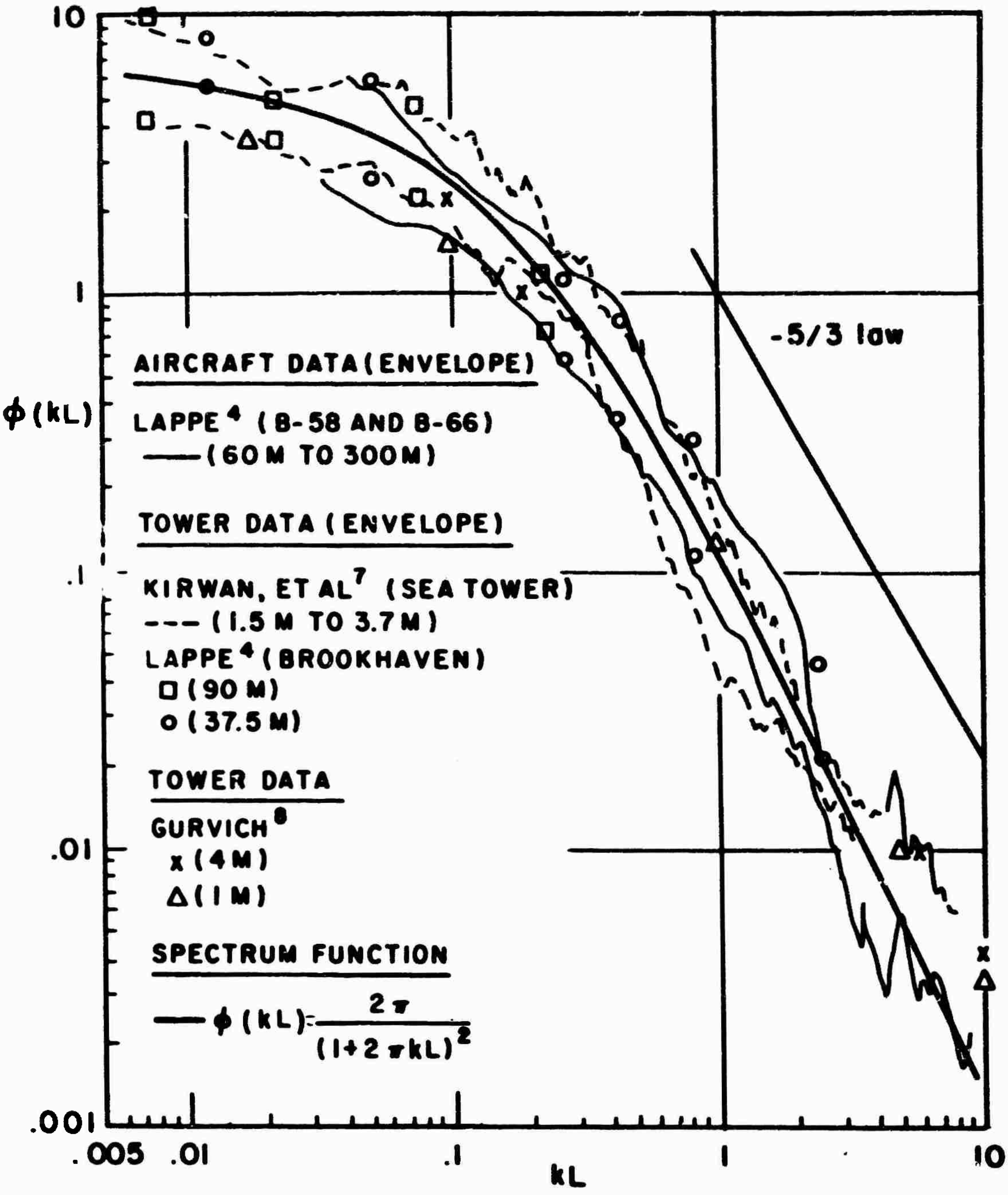

FIG. 1. VERTICAL VELOCITY SPECTRA PLOTTED NON-DIMENSIONALLY.

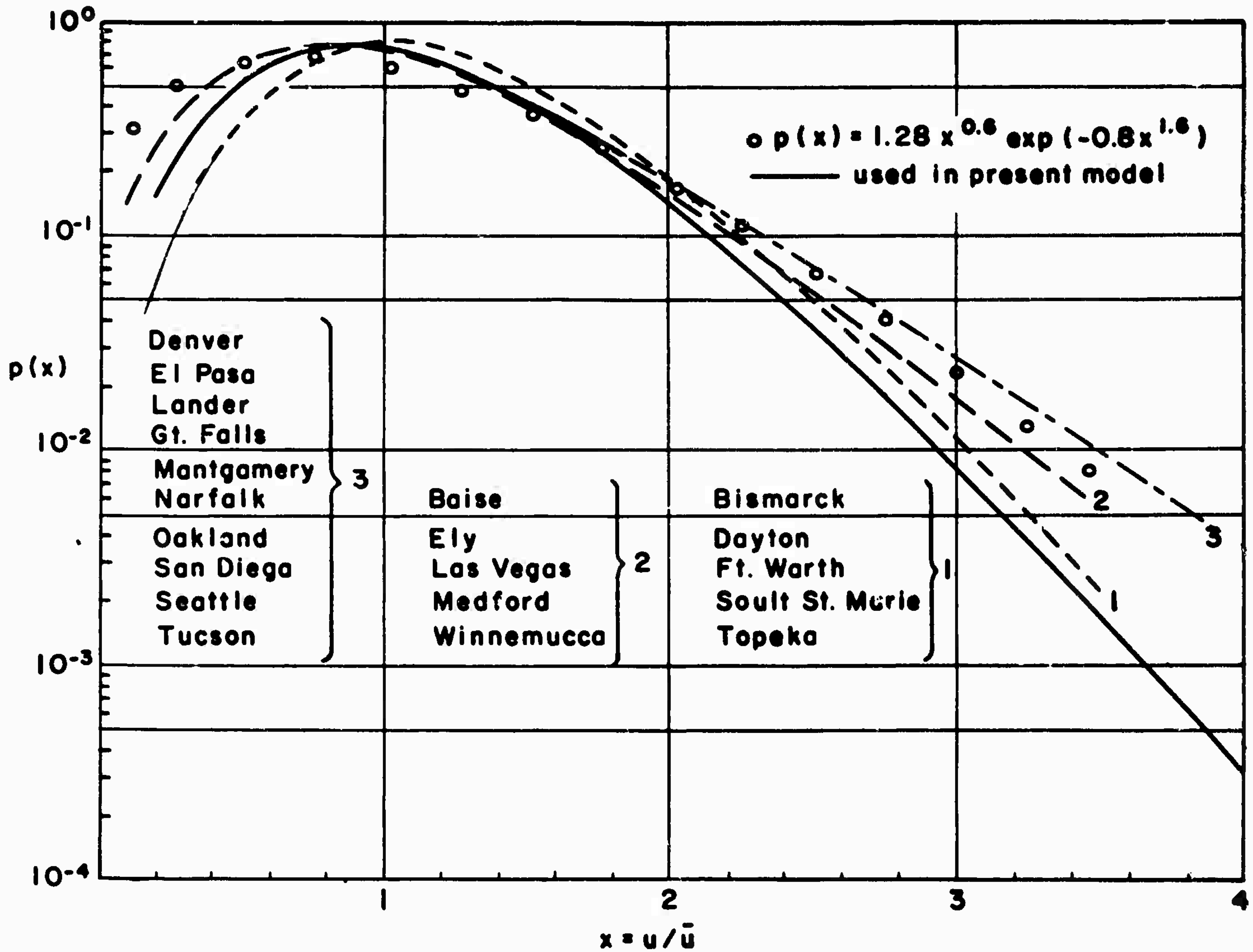

FIG. 2. WIND SPEED PROBABILITY DENSITY DISTRIBUTIONS FOR SMOOTH AND ROUGH TERRAINS.

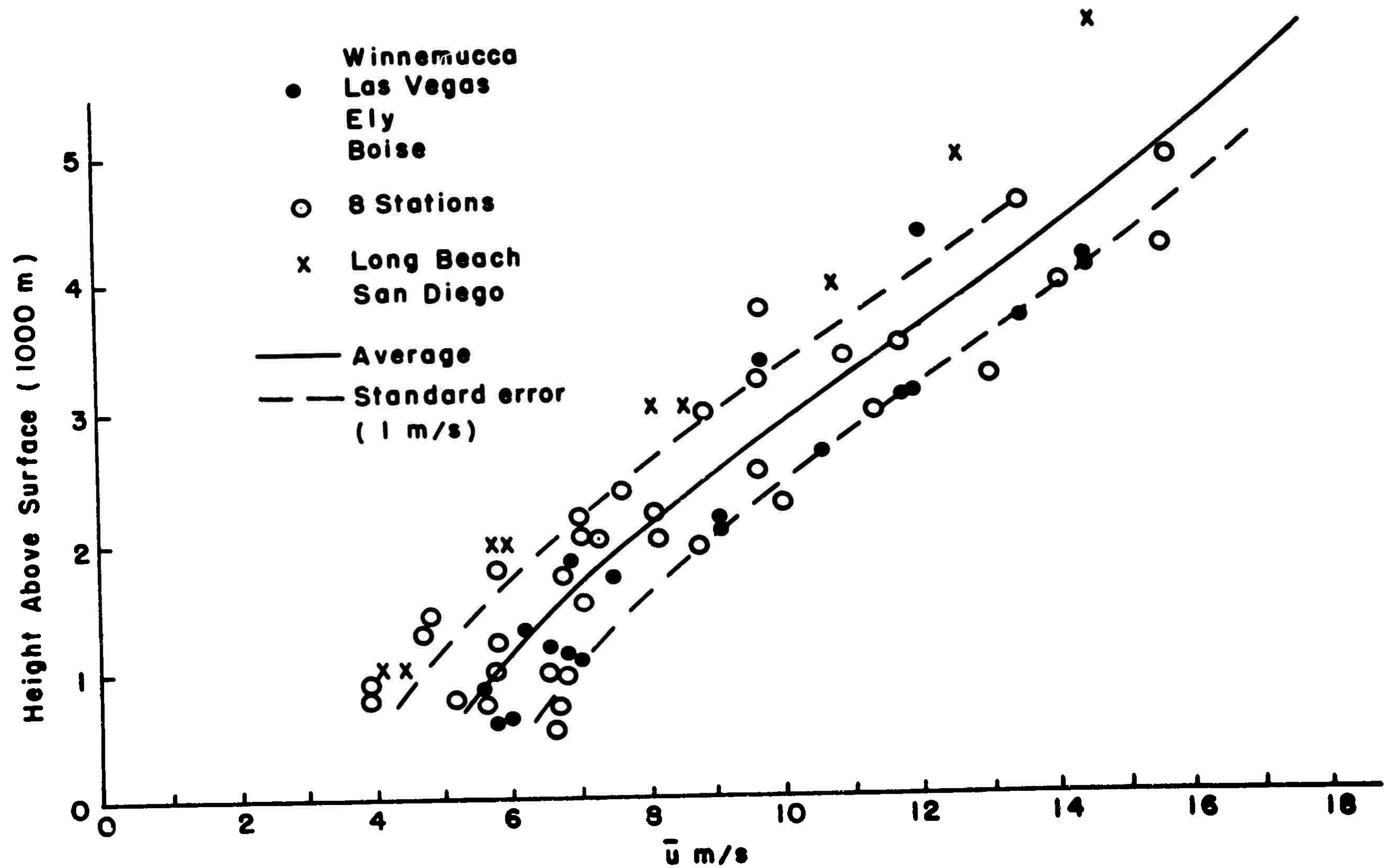

FIG. 3. CLIMATIC-WIND-SPEED AS A FUNCTION OF HEIGHT ABOVE THE SURFACE FOR ROUGH TERRAIN STATIONS.

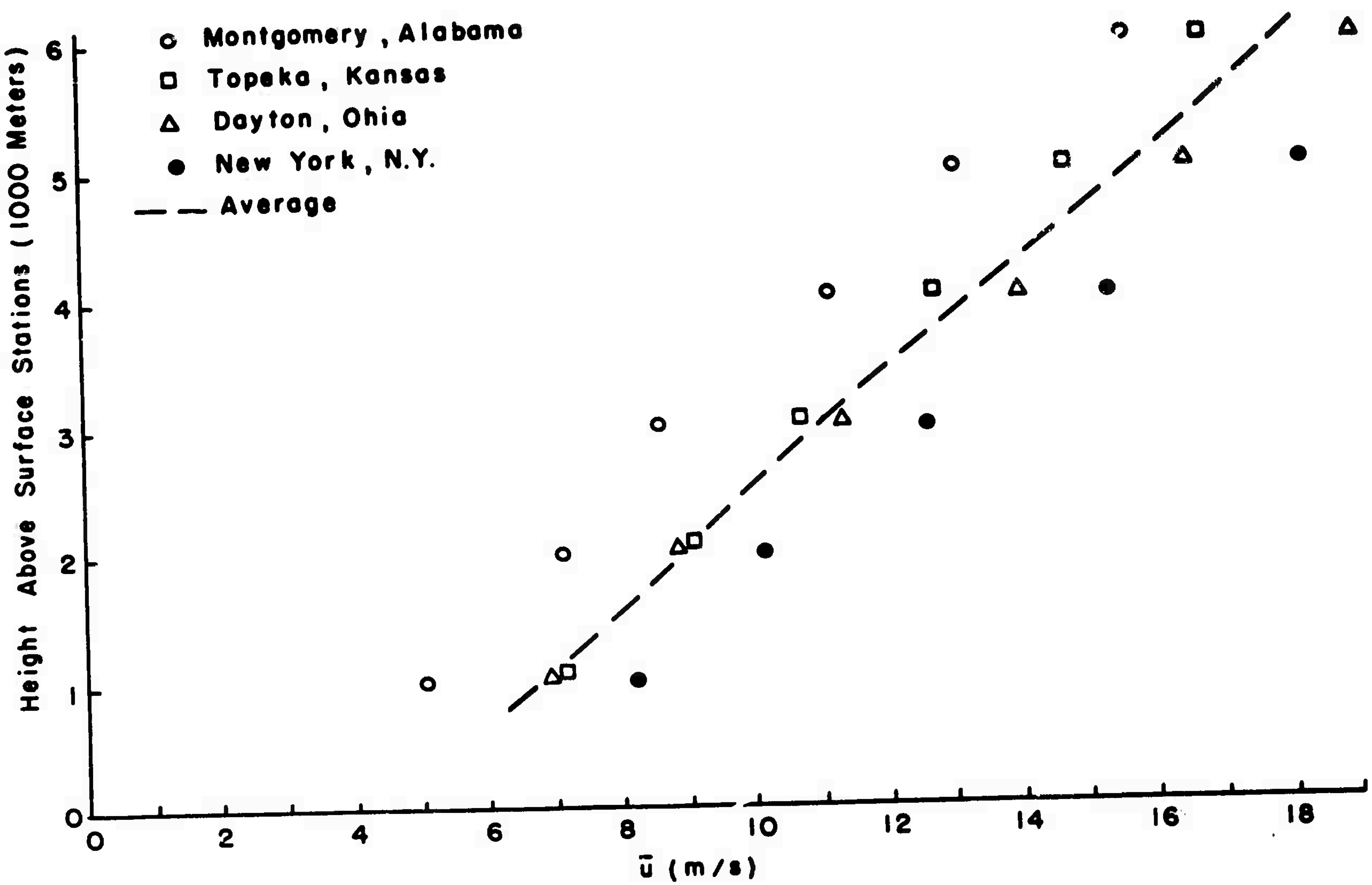

FIG. 4. CLIMATIC-WIND-SPEED AS A FUNCTION OF HEIGHT ABOVE THE SURFACE FOR SMOOTH TERRAIN STATIONS.

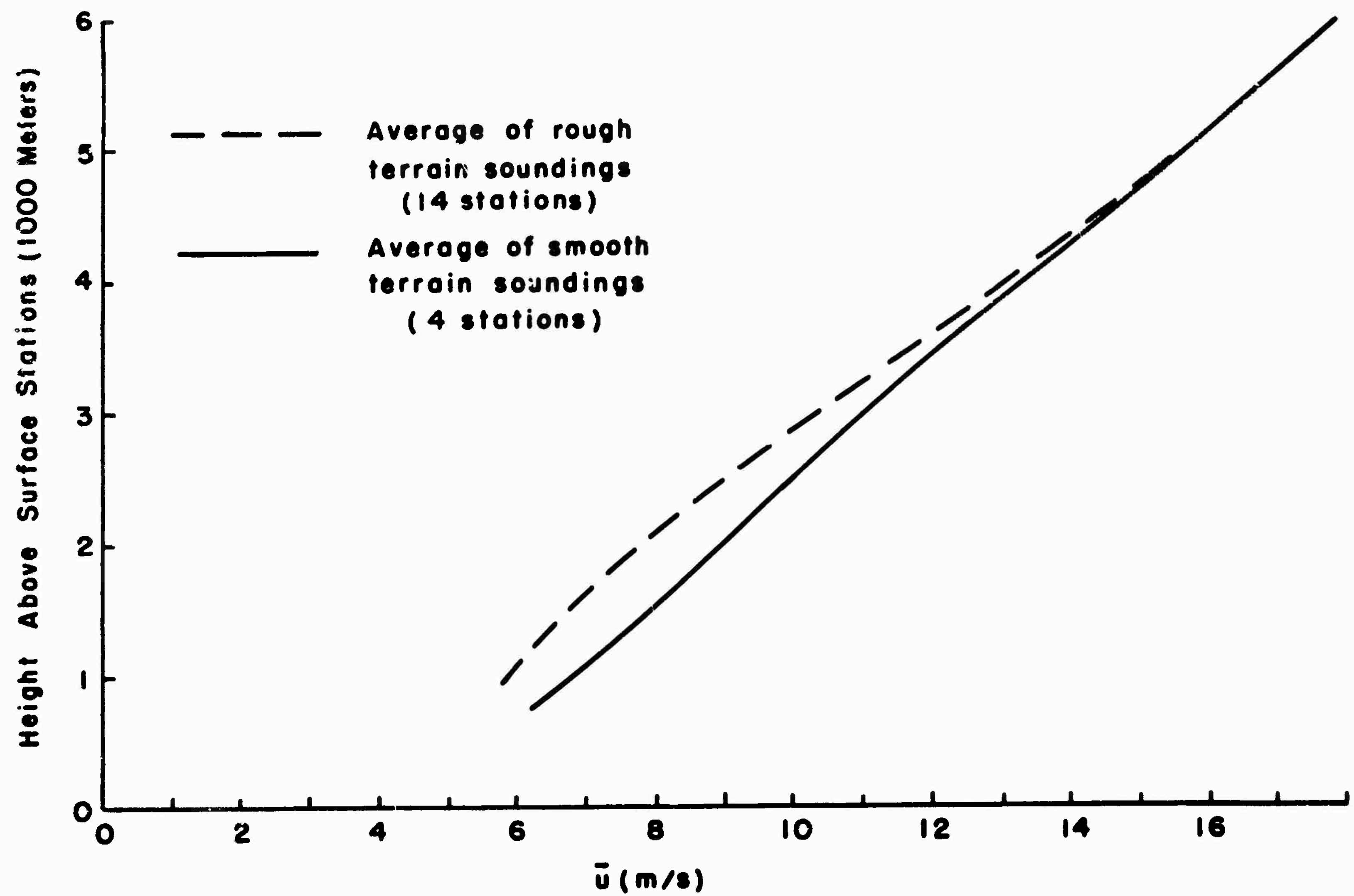

FIG. 5. COMPARISON OF CLIMATIC-WIND-SPEED AVERAGES.

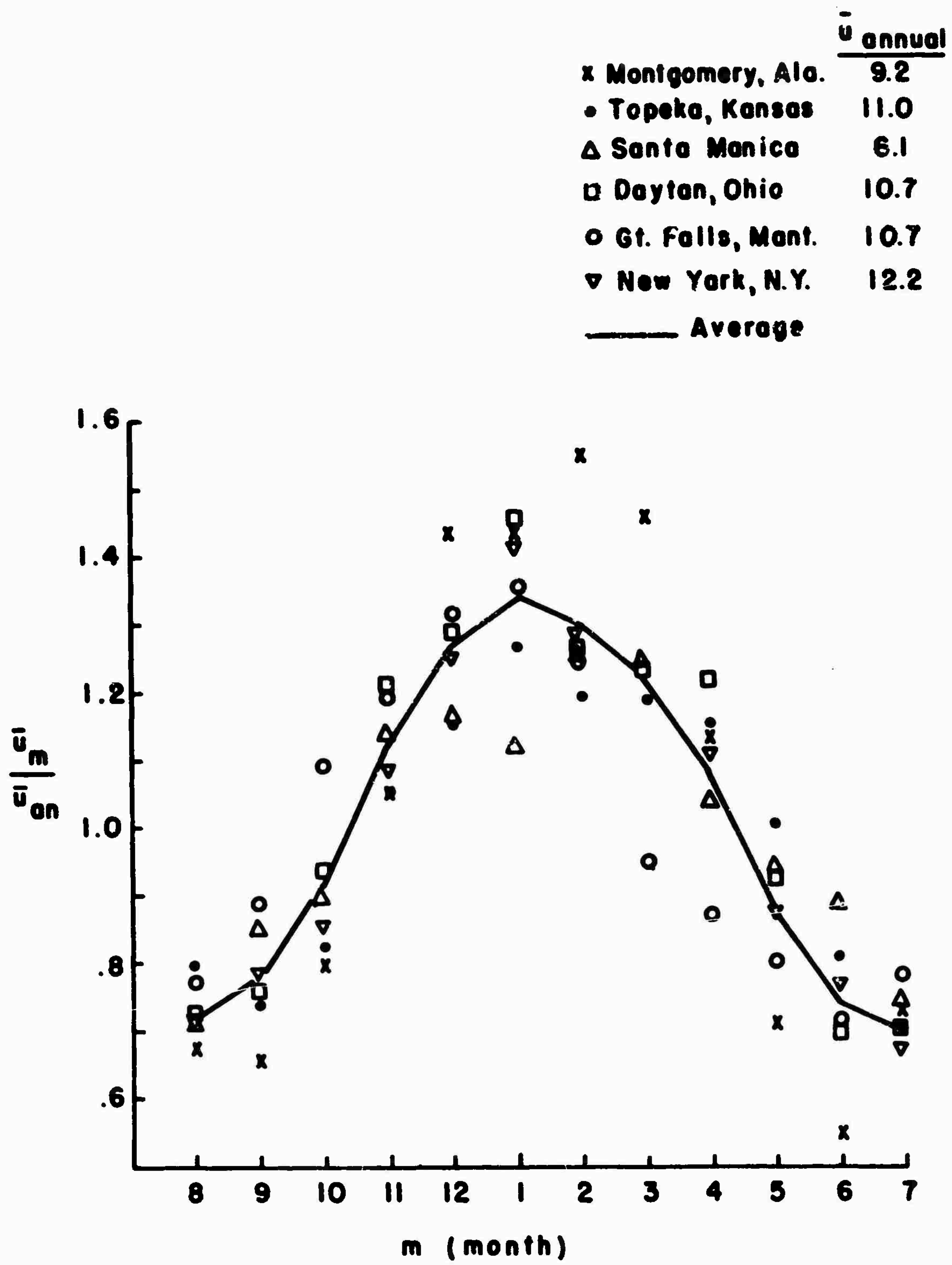

FIG. 6. MONTHLY-TO-YEARLY CLIMATIC-WIND-SPEED RATIOS AT THE 2000 M LEVEL FOR SIX SURFACE STATIONS

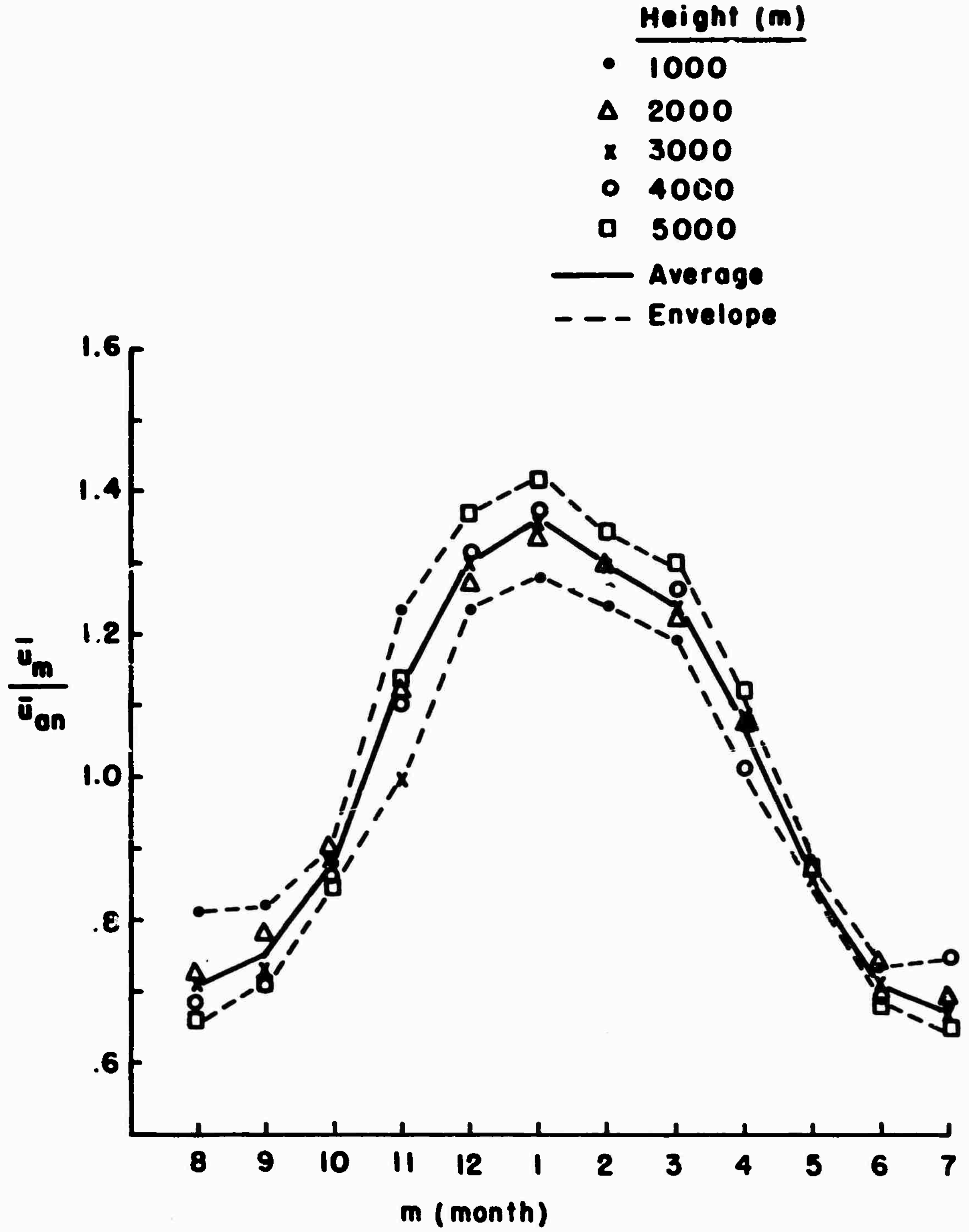

FIG. 7. MONTHLY-TO-YEARLY CLIMATIC-WIND-SPEED RATIO VALUES AVERAGED FOR SIX STATIONS AND FIVE LEVELS FROM 1000 TO 5000 M ABOVE THE SURFACE STATIONS.

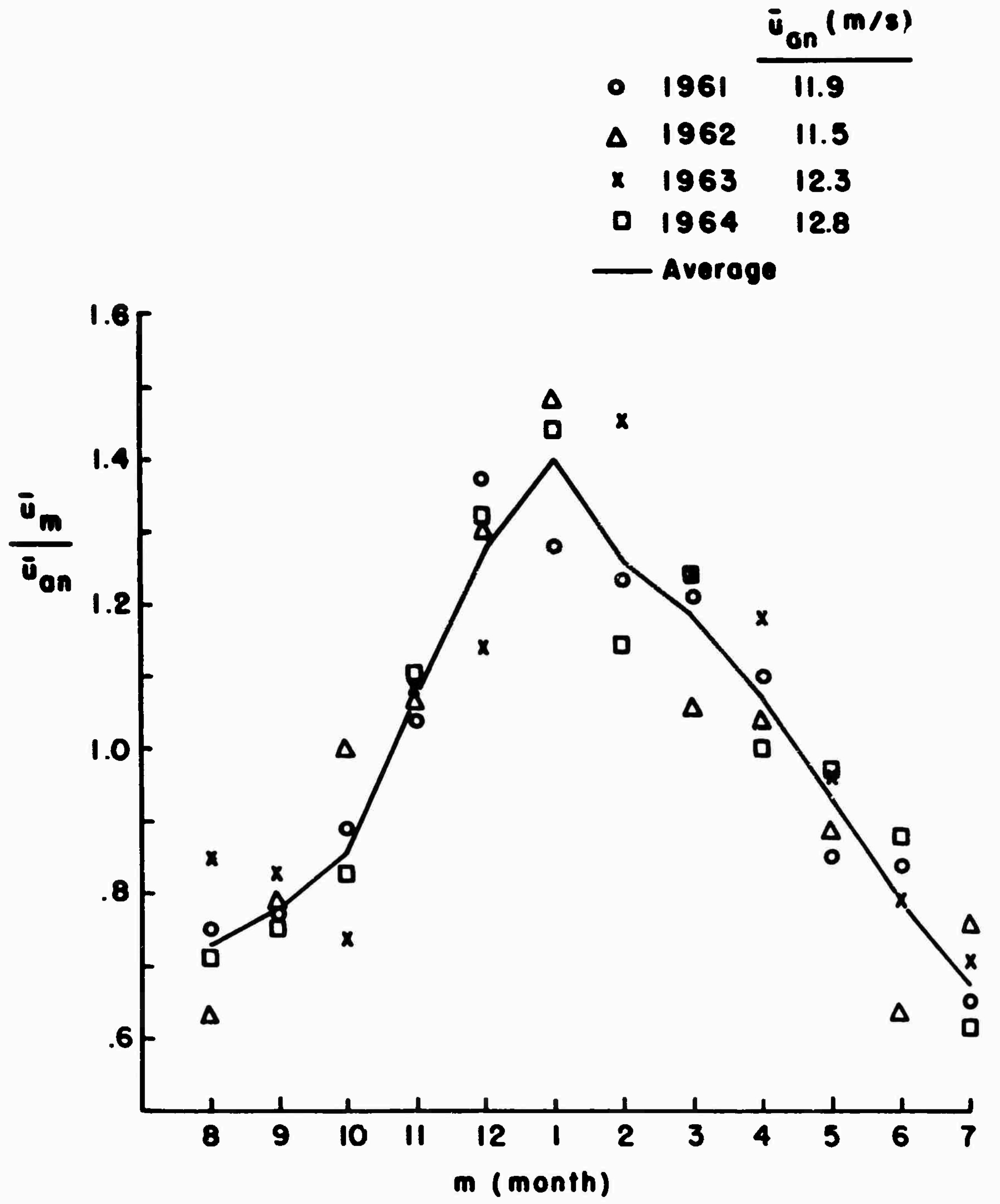

FIG. 8. MONTHLY-TO-YEARLY CLIMATIC-WIND-SPEED RATIOS FOR FOUR YEARS AT 2000 M ABOVE THE NEW YORK STATION (READINGS AT 1300 LST).

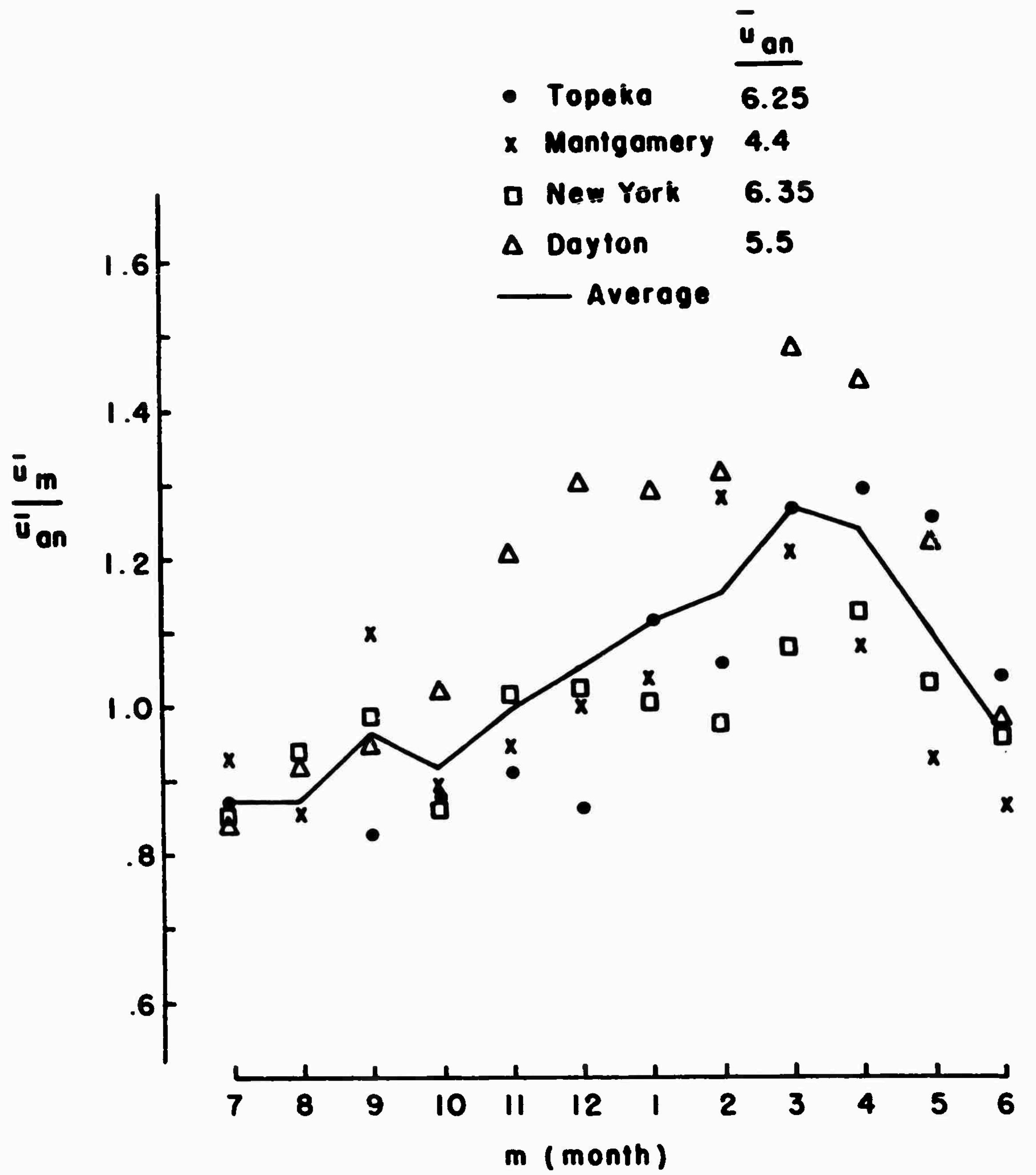

FIG. 9. MONTHLY-TO-YEARLY CLIMATIC-WIND-SPEED RATIOS AT THE SURFACE FOR FOUR SMOOTH TERRAIN STATIONS.

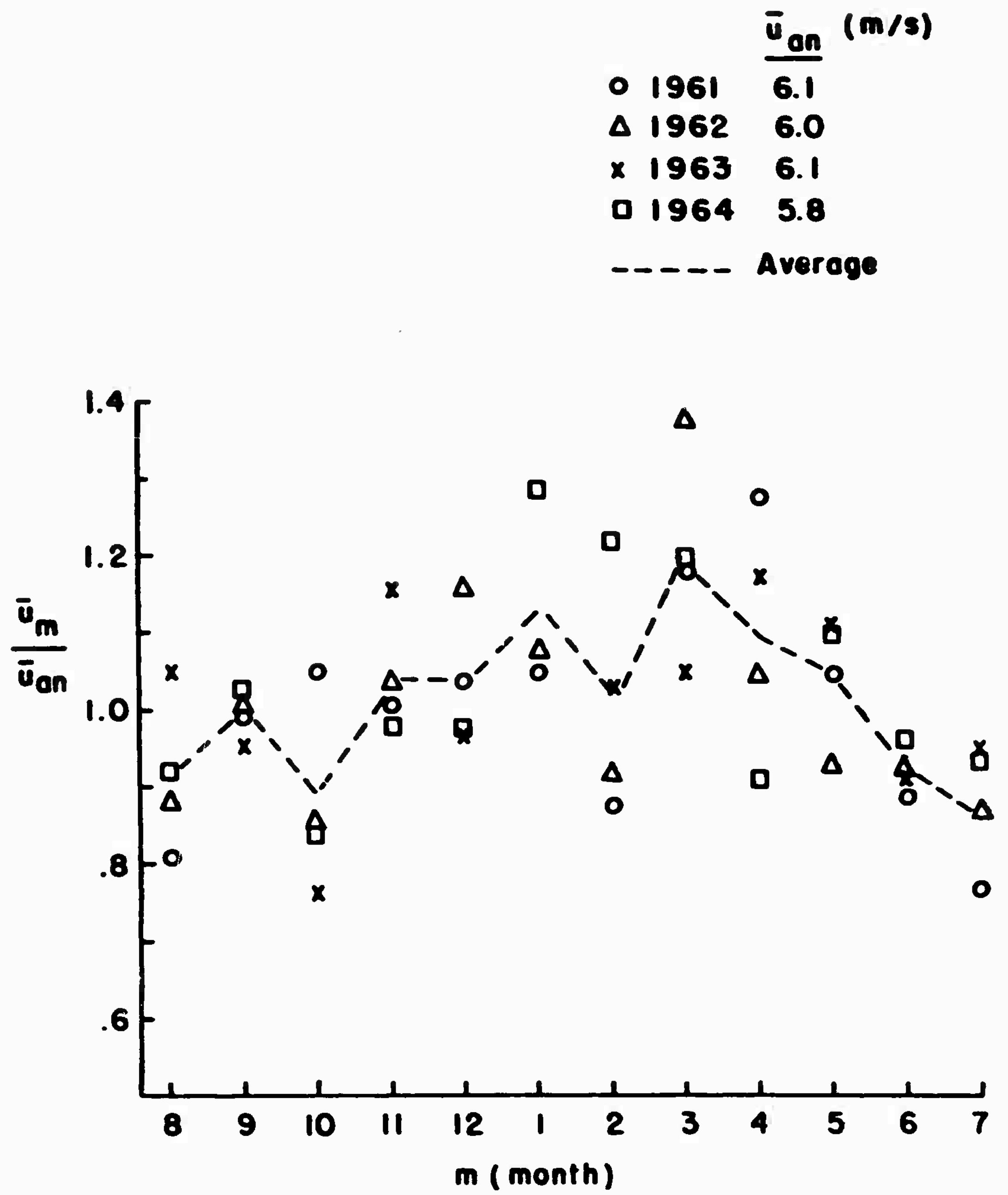

FIG. 10. MONTHLY-TO-YEARLY CLIMATIC-WIND-SPEED RATIOS FOR FOUR YEARS NEAR THE SURFACE FOR NEW YORK (OBSERVATIONS OBTAINED AT 1900 LST).

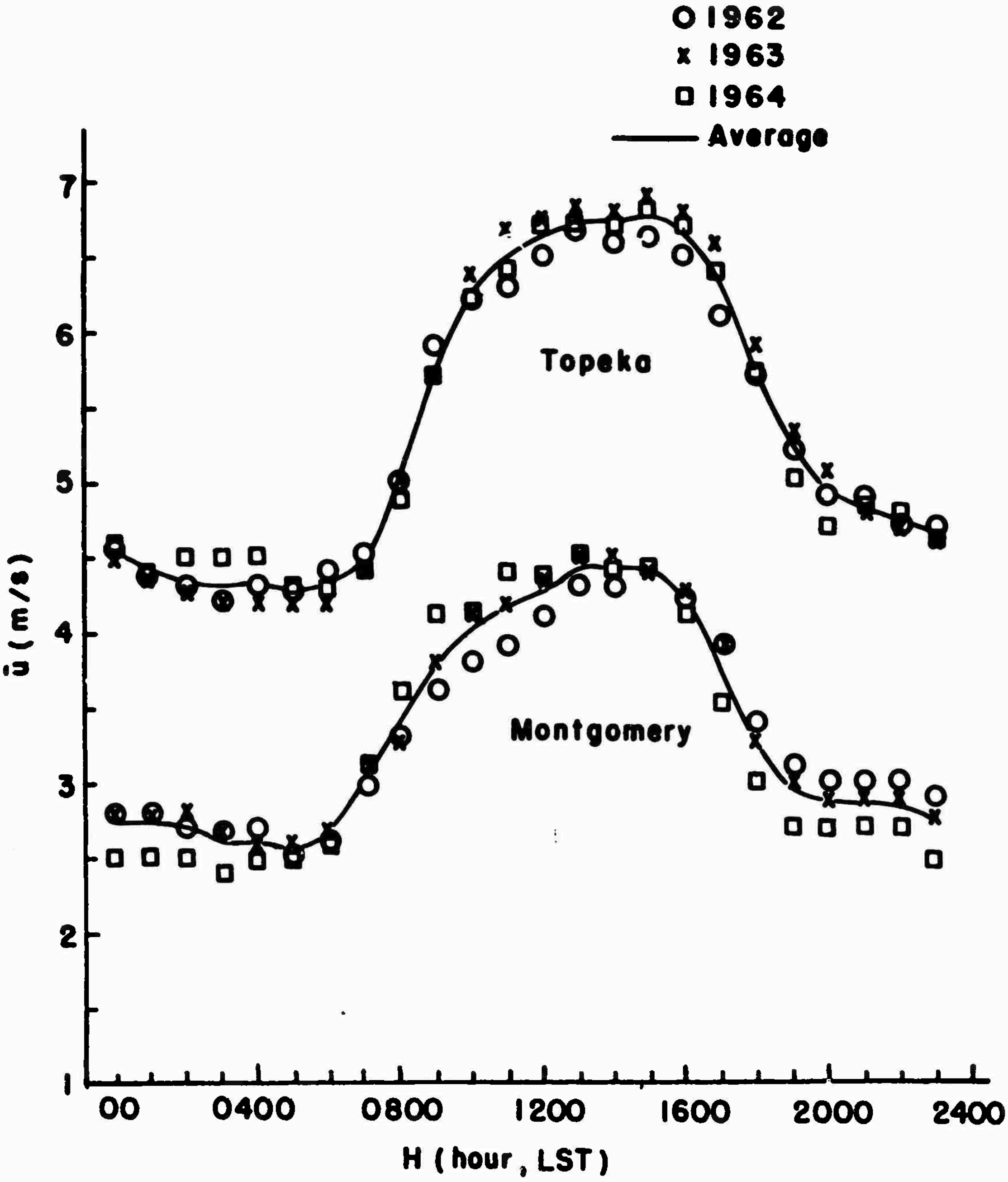

FIG. 11. HOURLY CLIMATIC-WIND-SPEED VALUES NEAR THE SURFACE FOR TOPEKA, KANSAS AND MONTGOMERY, ALABAMA FOR 1962-1964.

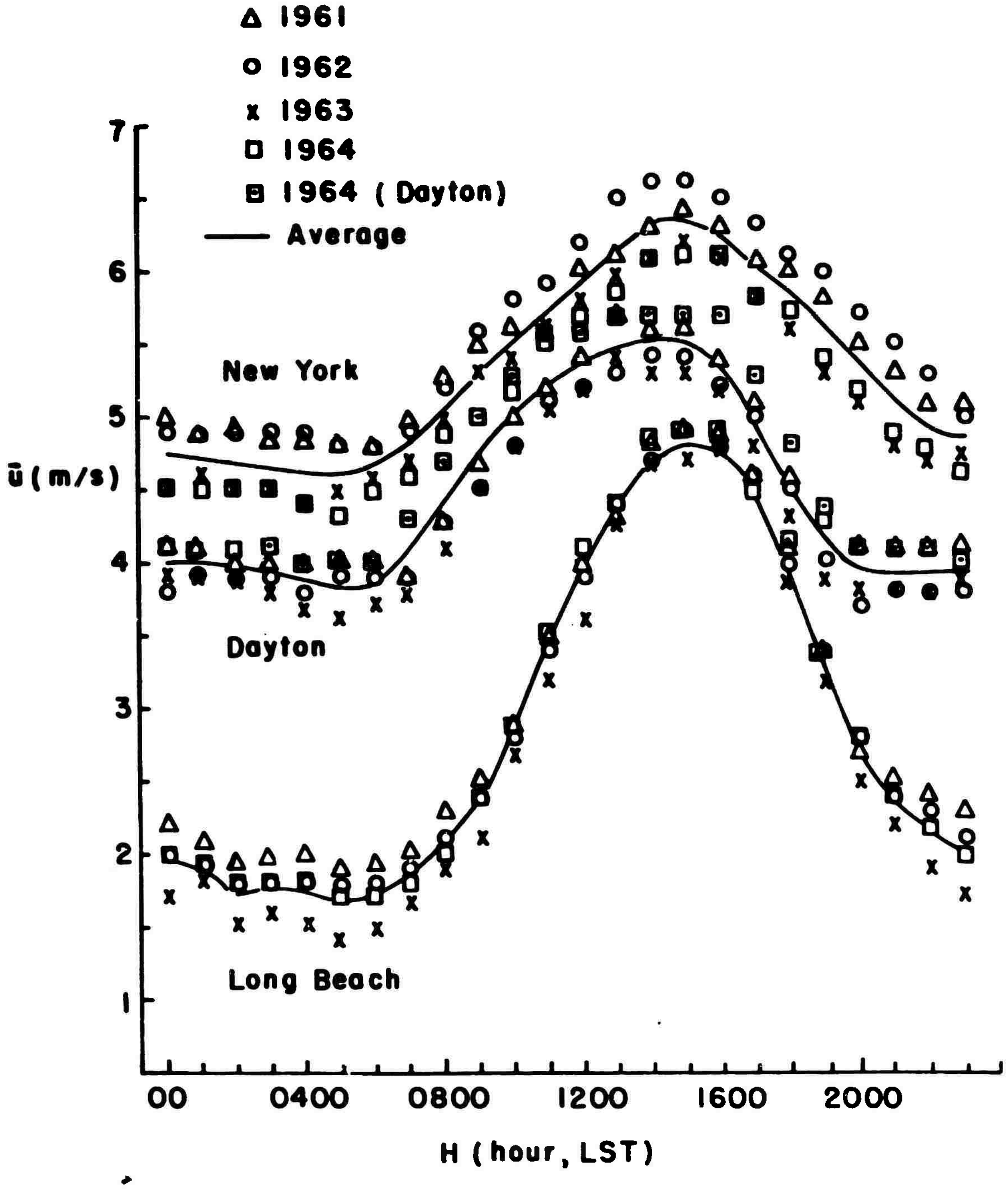

FIG. 12. HOURLY CLIMATIC-WIND-SPEED VALUES NEAR THE SURFACE FOR NEW YORK, N. Y.; DAYTON, OHIO; AND LONG BEACH, CALIFORNIA FOR 1961-1964.

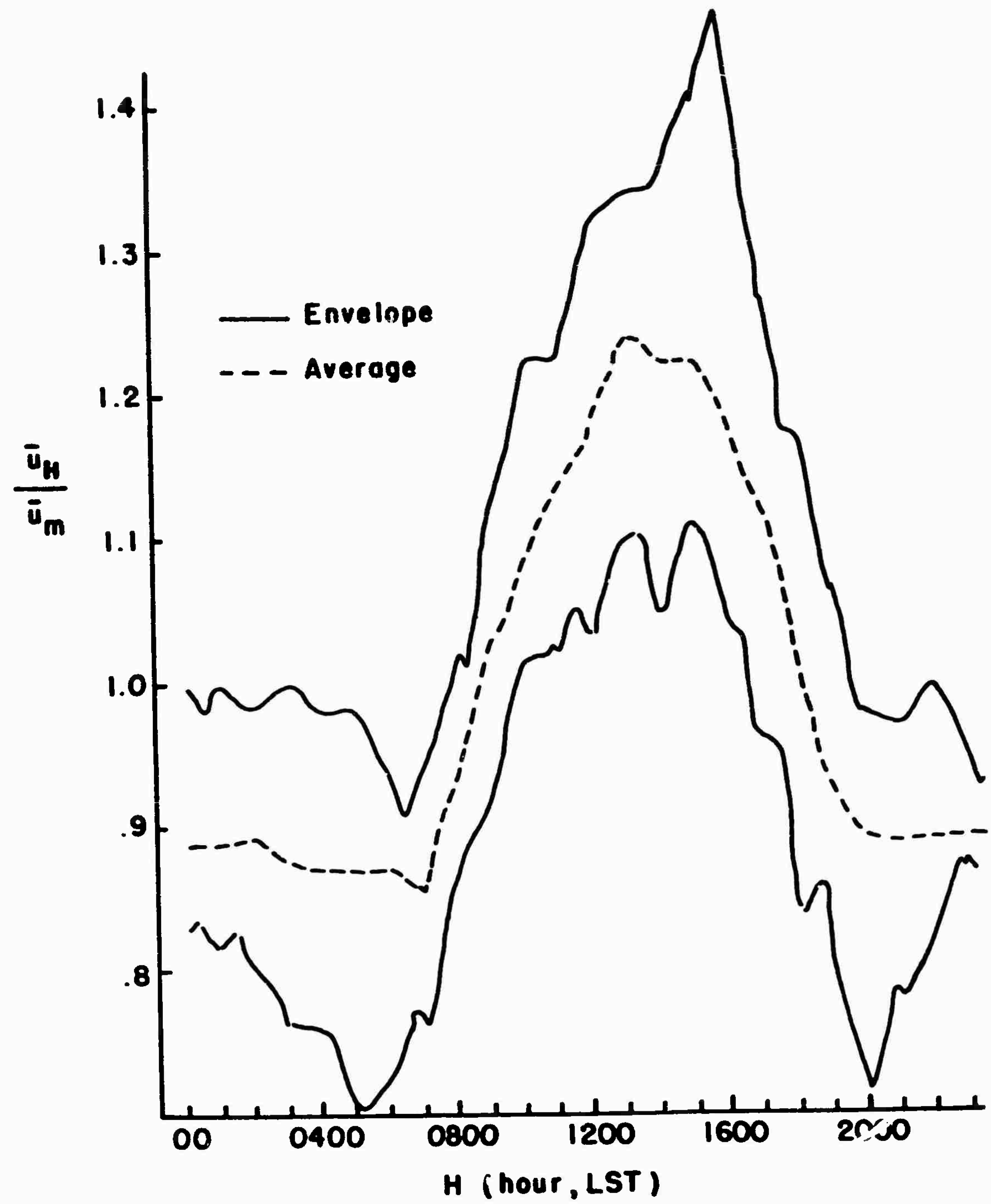

FIG. 13. ENVELOPE OF HOURLY-TO-MONTHLY CLIMATIC-WIND-SPEED RATIOS NEAR THE SURFACE FOR DAYTON, OHIO FOR 1961.

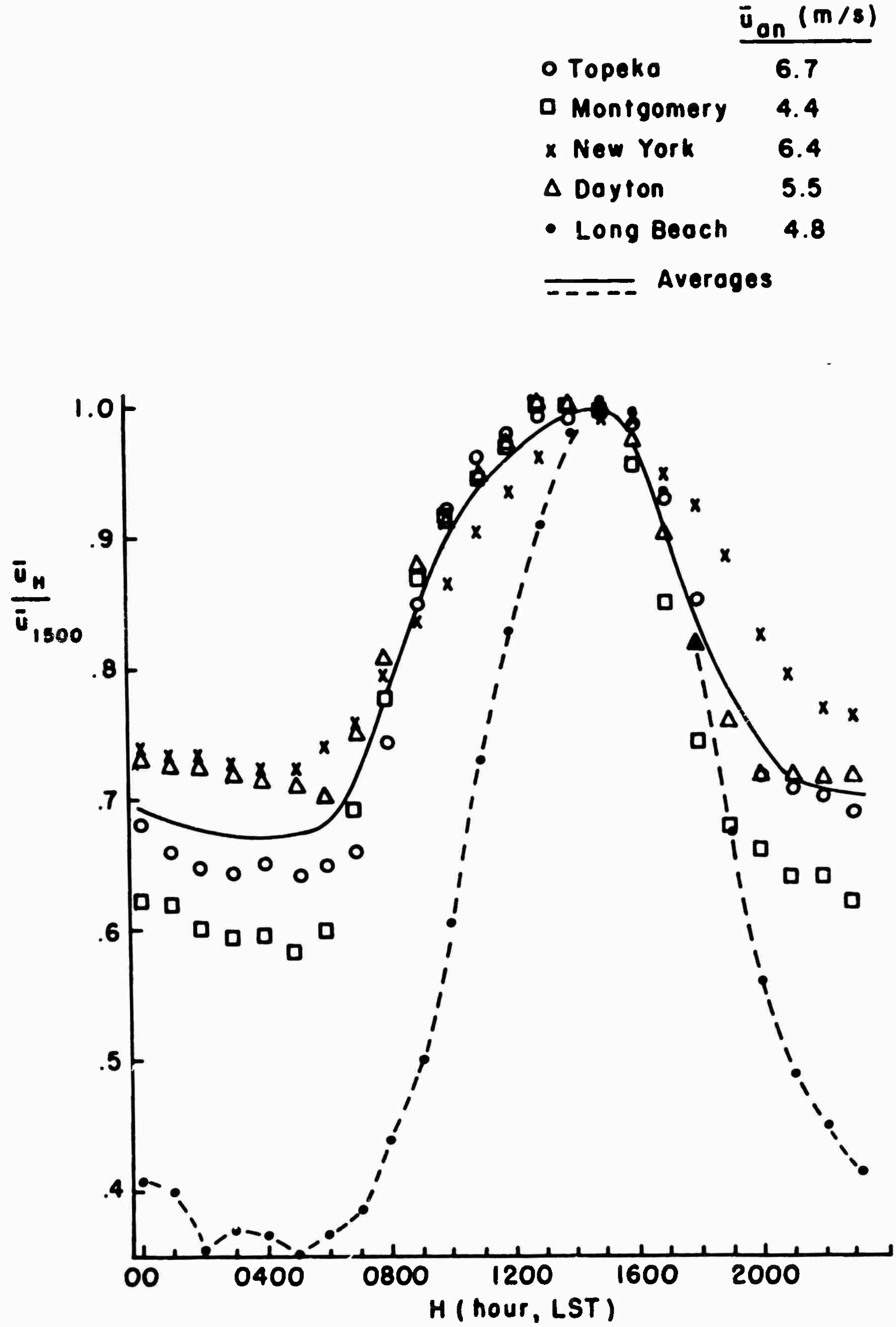

FIG. 14. HOURLY-TO-MAXIMUM HOURLY CLIMATIC-WIND-SPEED RATIOS NEAR THE SURFACE FOR FIVE STATIONS.

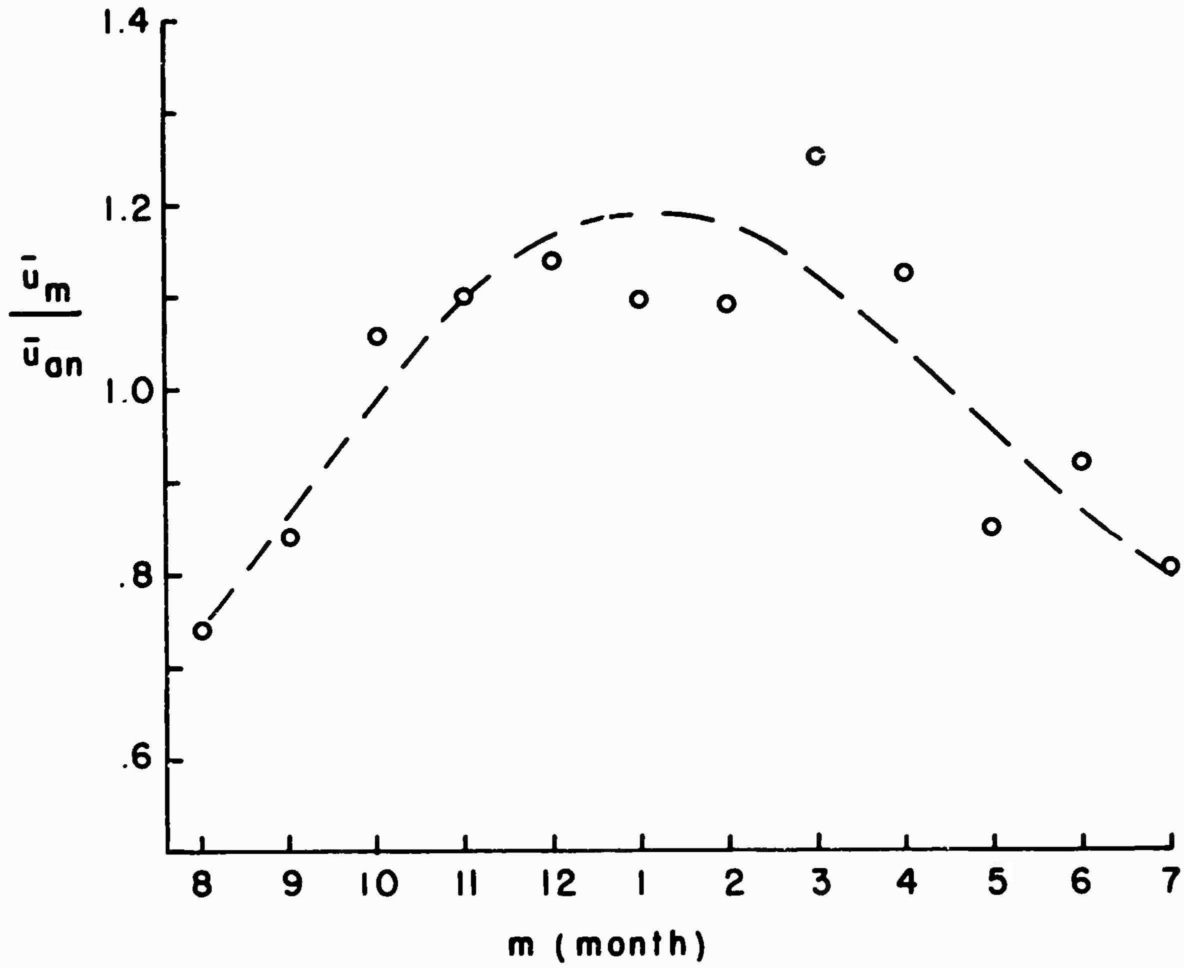

FIG. 15. MONTHLY-TO-YEARLY CLIMATIC-WIND-SPEED RATIOS AT 300 M FOR STABLE CONDITIONS OVER SMOOTH TERRAINS.

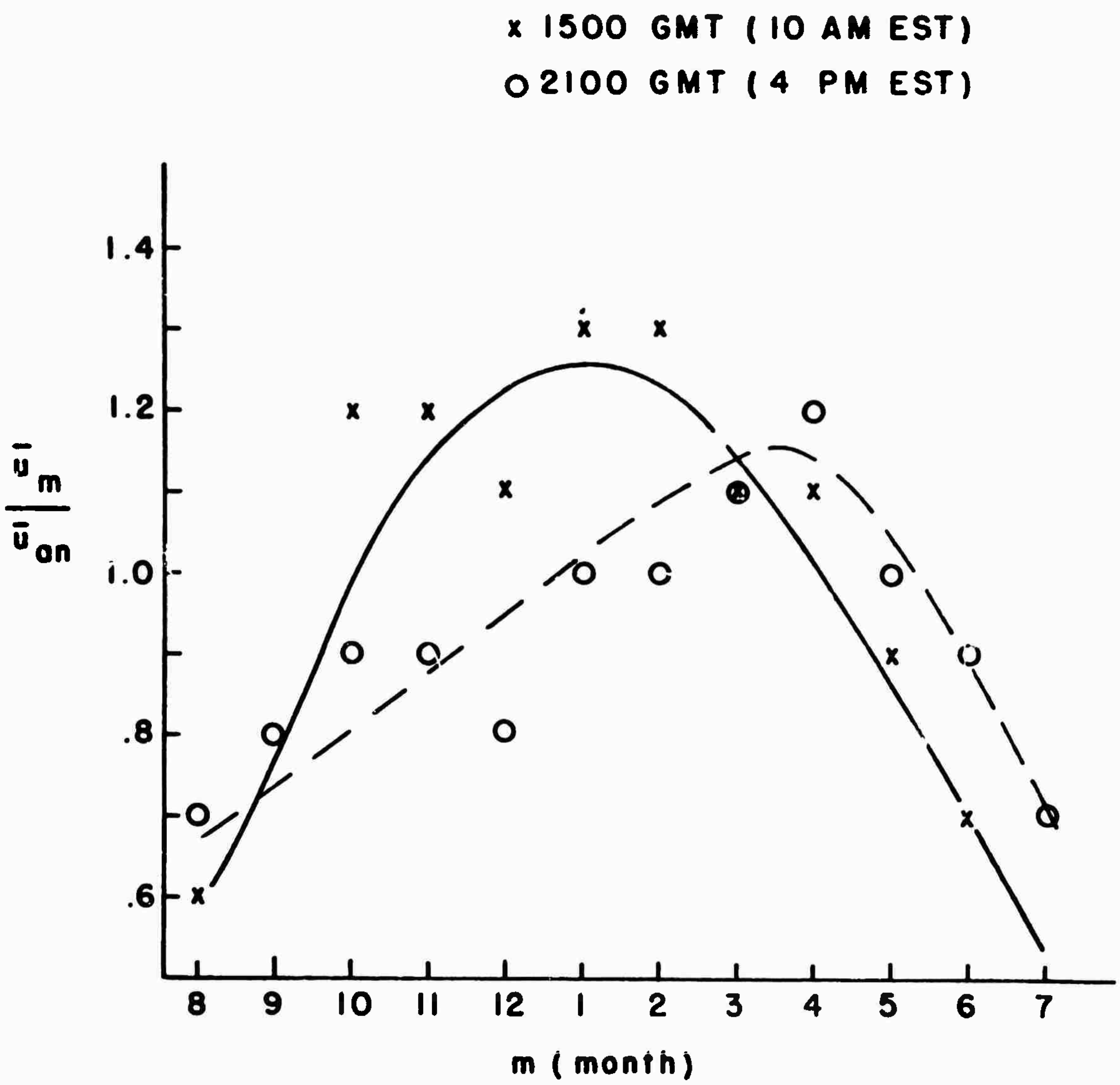

FIG. 16. MONTHLY-TO-YEARLY CLIMATIC-WIND-SPEED RATIOS AT 300 M FOR UNSTABLE CONDITIONS OVER SMOOTH TERRAINS (FOR 1500 AND 2100 LST).

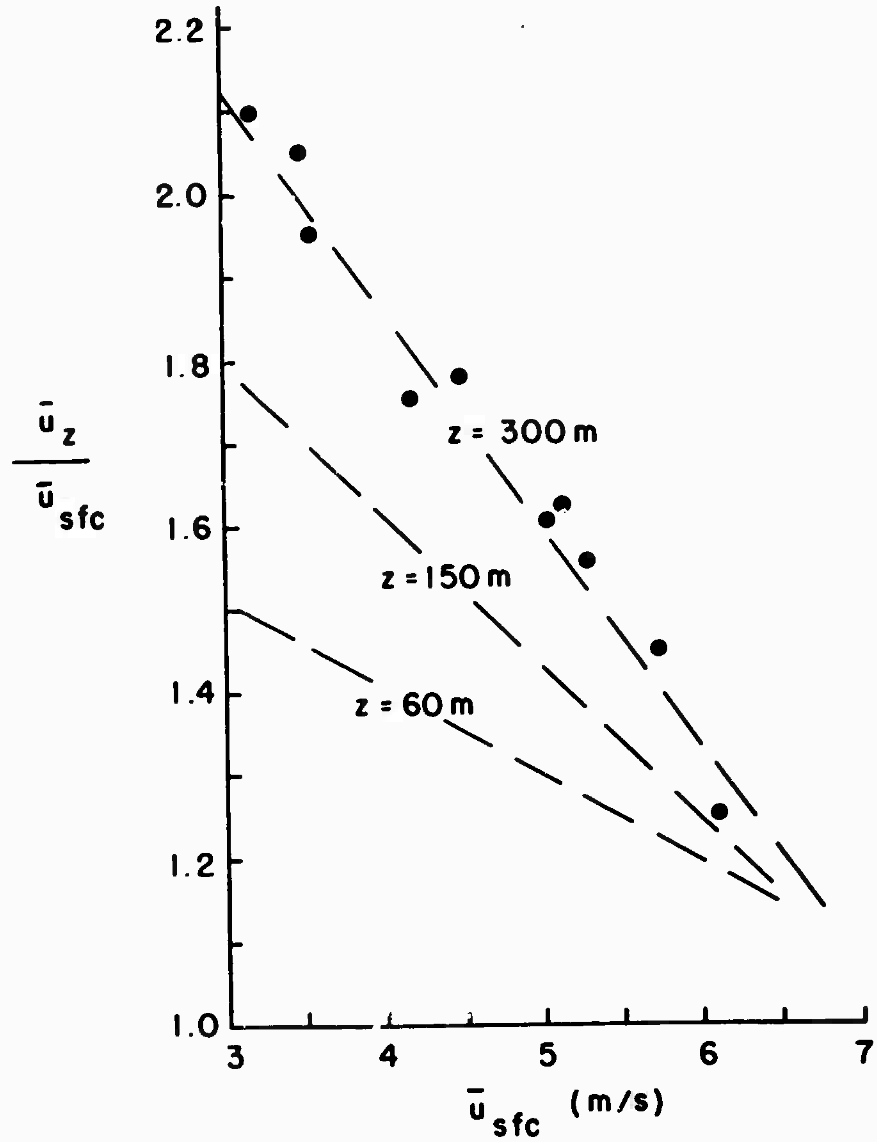

FIG. 17. CLIMATIC-WIND-SPEED RATIOS $\bar{u}_z/\bar{u}_{sfc}$ FOR STABLE CONDITIONS OVER SMOOTH TERRAINS.

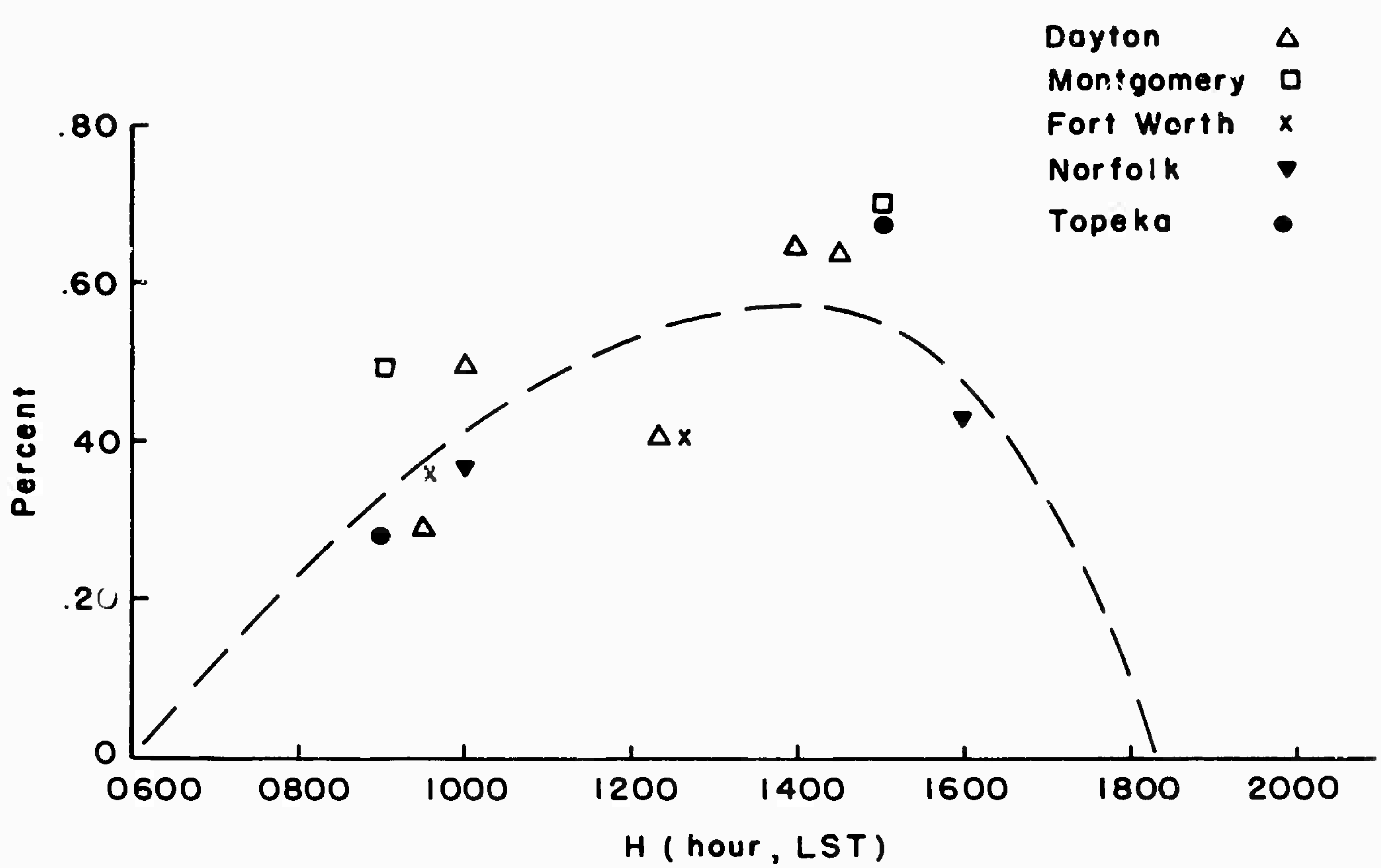

FIG. 18. VARIATION OF UNSTABLE (INCLUDING NEUTRAL) STABILITY CONDITIONS FOR DAYTIME HOURS.

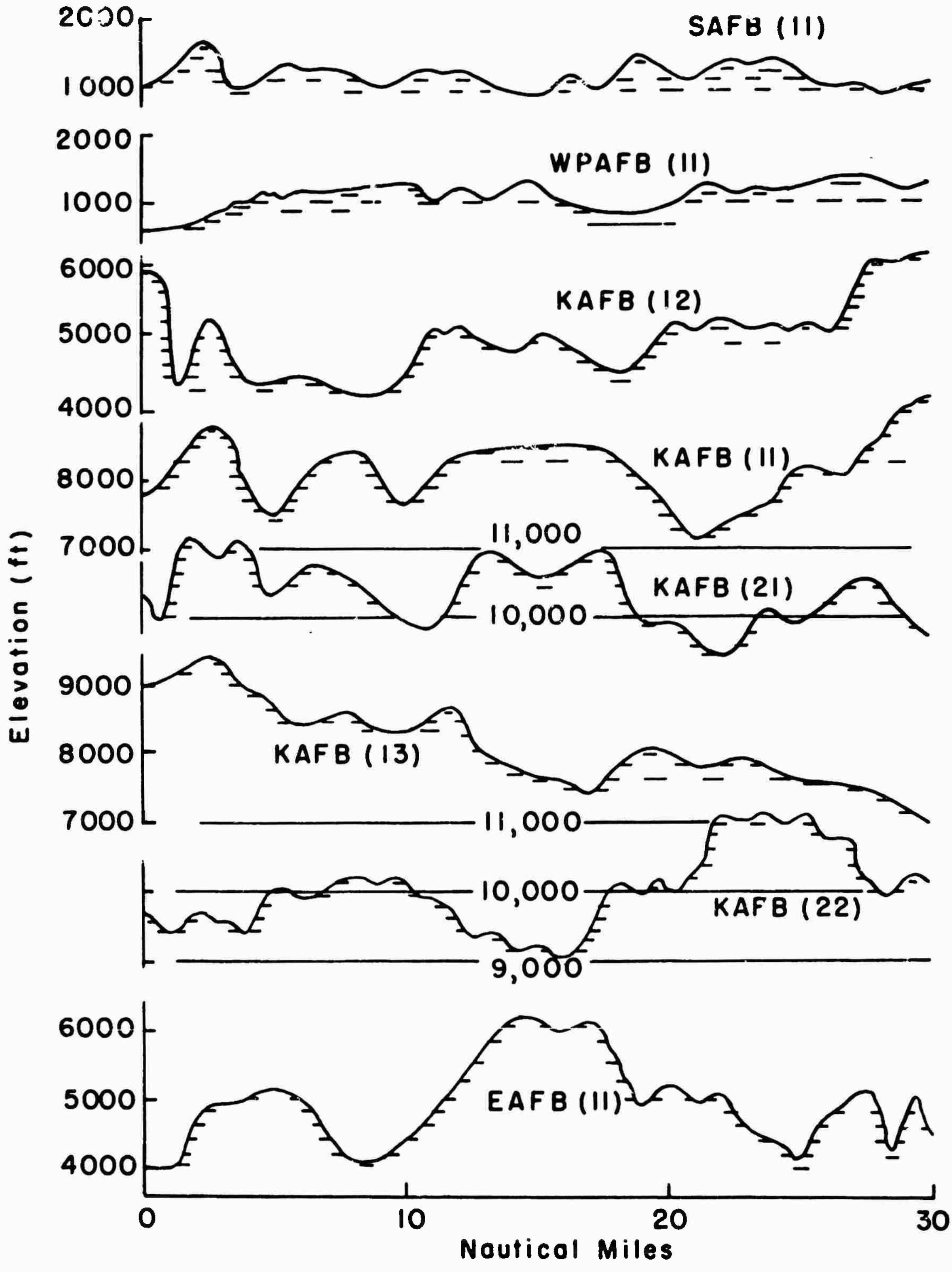

FIG. 19. TERRAIN PROFILES FOR B-66 FLIGHT TRACKS
(a) LOW MOUNTAIN PROFILES

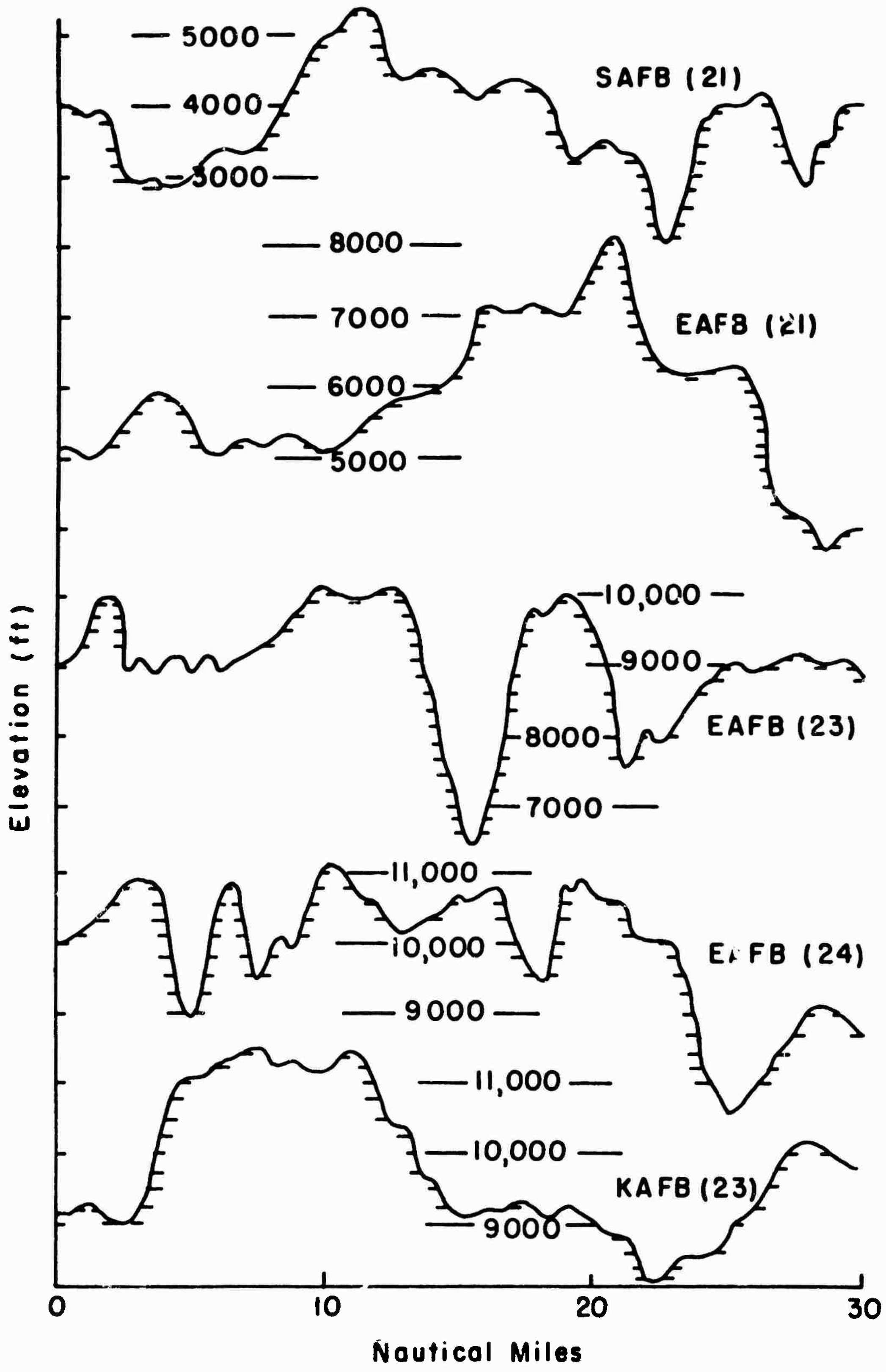

(b) HIGH MOUNTAIN PROFILES

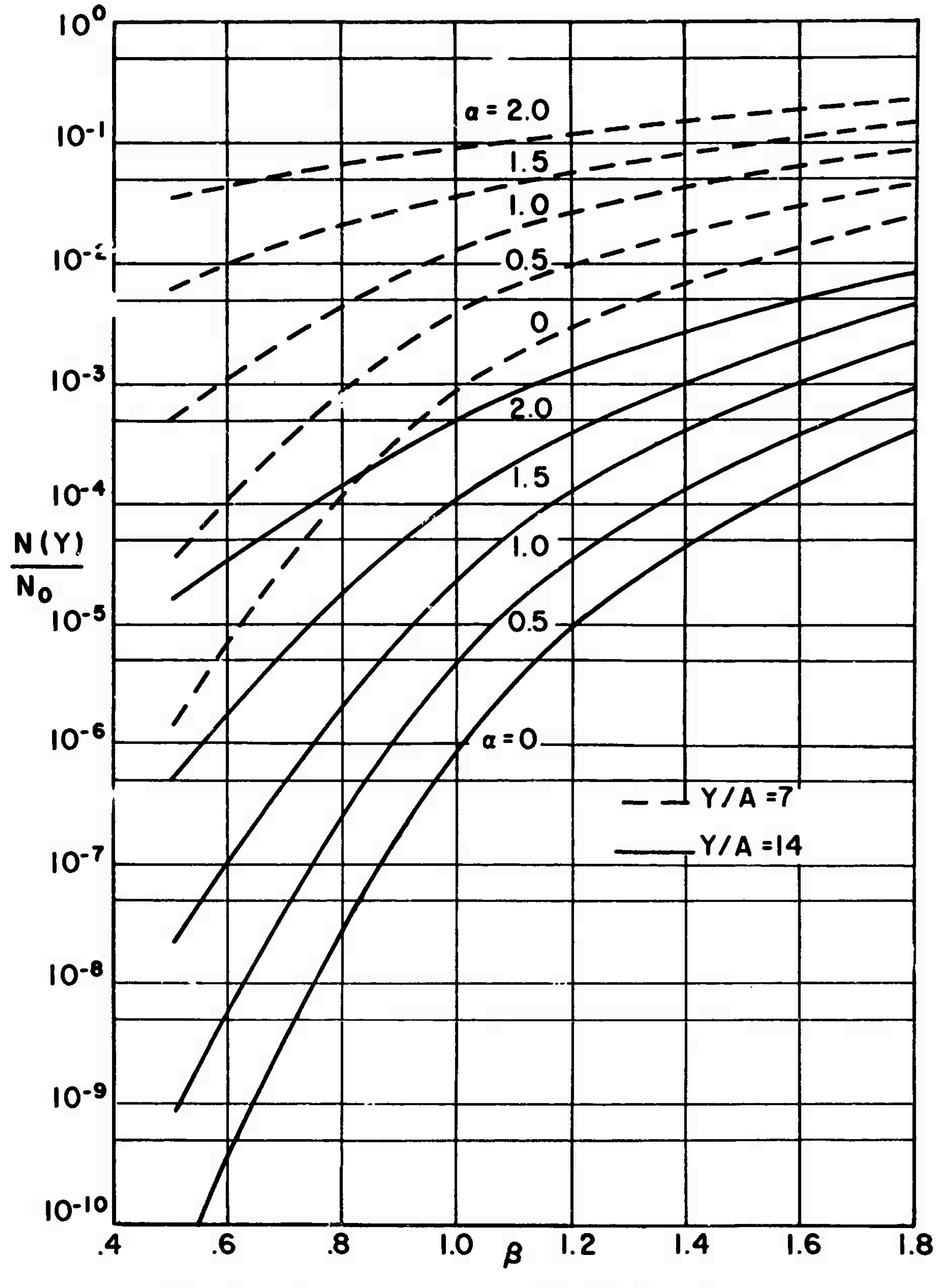

FIG. 20. GENERALIZED LOAD EXCEEDANCE CURVES

(a) Y/A = 7; Y/A = 14

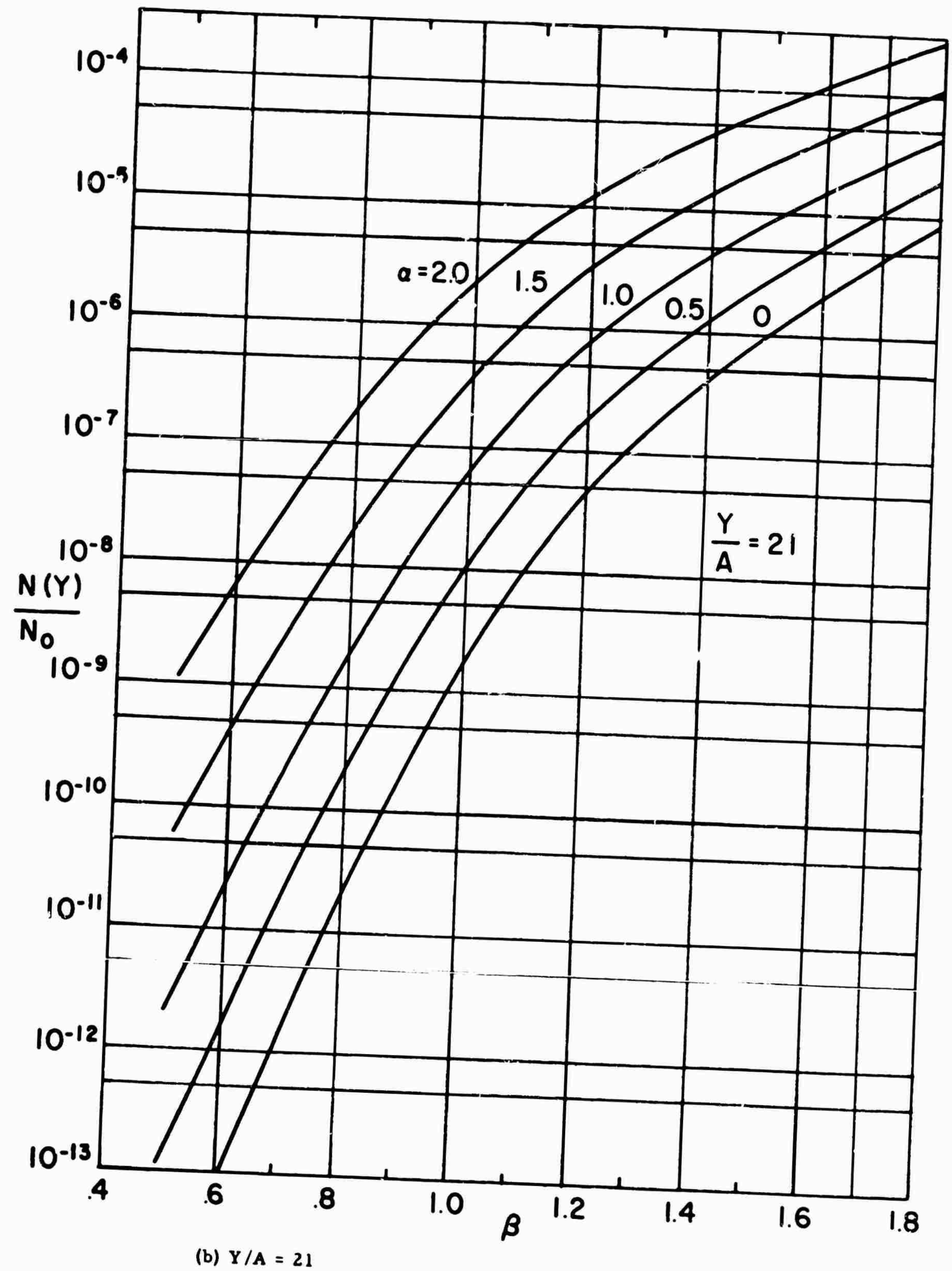

10-4
10-5
10-6
10-7
10-8
10-9
10-10
10-11
10-12
10-13
N(Y)/N0
α = 2.0
1.5
1.0
0.5
0
Y/A = 21
.4
.6
.8
1.0
1.2
1.4
1.6
1.8
β

(b) Y/A = 21

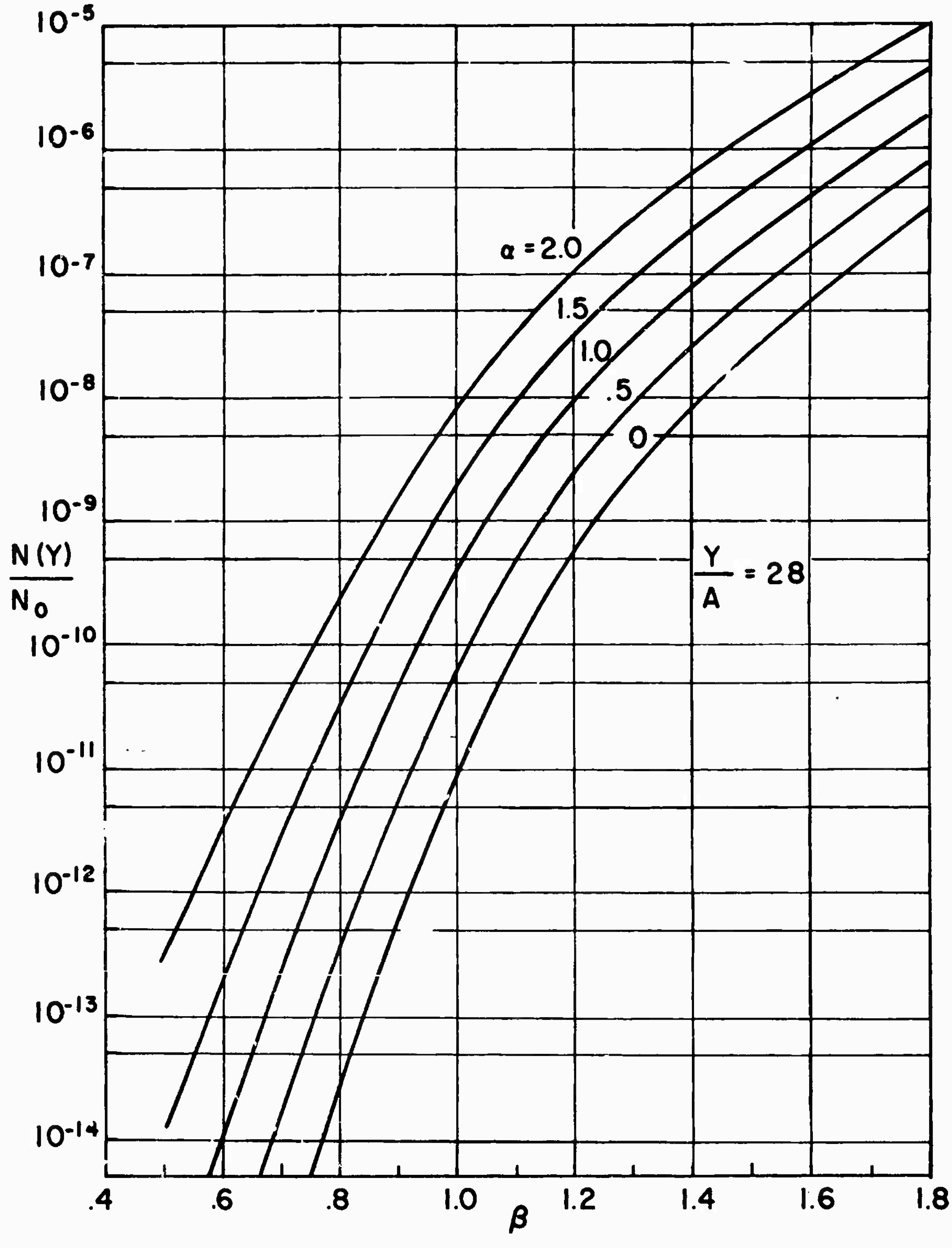

10^{-5}
10^{-6}
10^{-7}
10^{-8}
10^{-9}
$\frac{N(Y)}{N_0}$
10^{-10}
10^{-11}
10^{-12}
10^{-13}
10^{-14}
$\alpha = 2.0$
1.5
1.0
.5
0
$\frac{Y}{A} = 28$
.4
.6
.8
1.0
1.2
1.4
1.6
1.8
β

(c) Y/A = 28

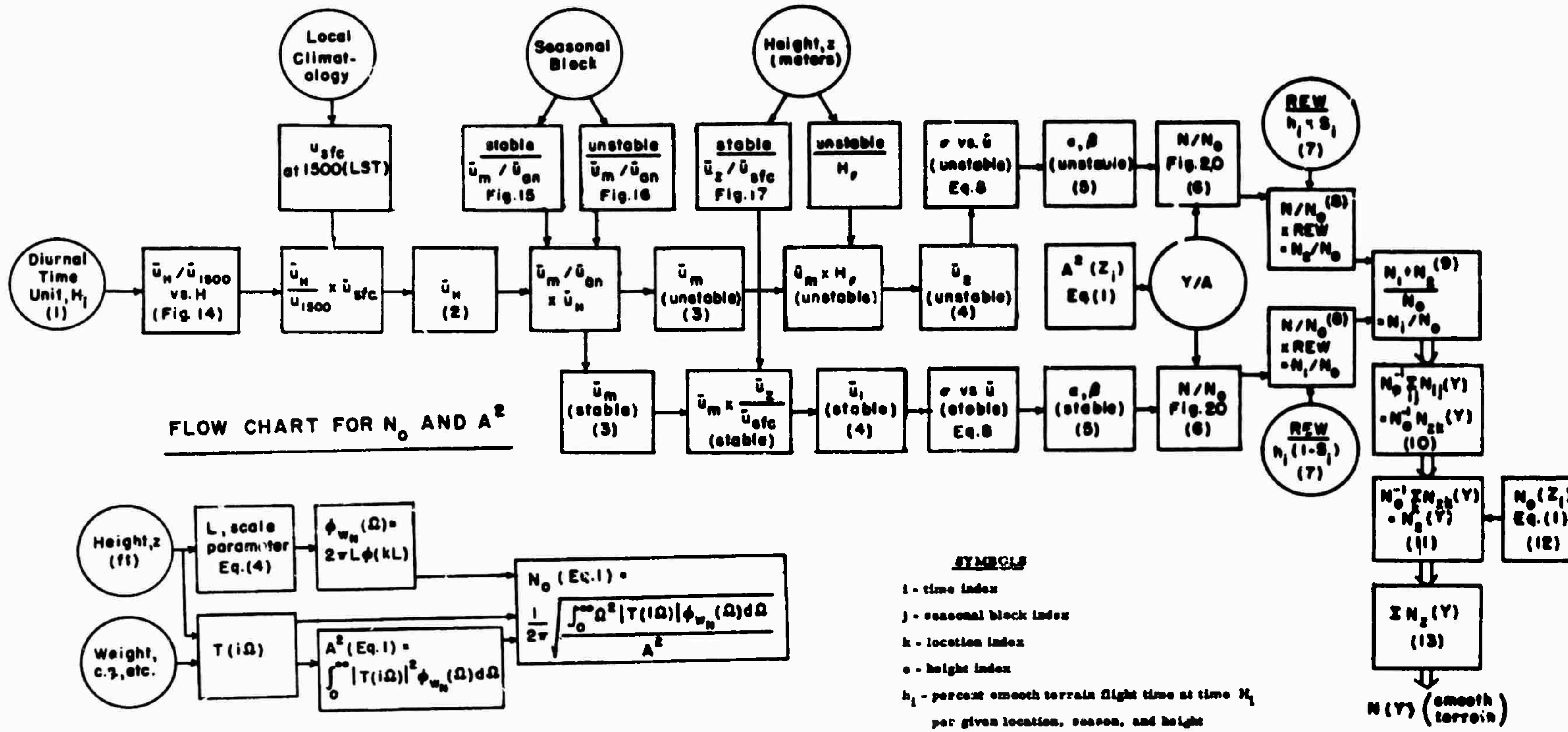

SYMBOLS

i - time index

j - seasonal block index

k - location index

z - height index

h_i - percent smooth terrain flight time at time H_i per given location, season, and height

s_i - percent unstable conditions for H_i (Figure 18)

H_F - height factor for unstable conditions (1.5 @ 300 m and 1.35 @ 60 m)

REW - relative exposure weight

NOTES

- Circles represent selected input conditions; squares represent model characteristics and outputs.
- Numbers in parenthesis refer to steps described in Section 8.

FIG. 21. FLOW CHART OF MODEL APPLICATION FOR SMOOTH TERRAIN CONDITION.

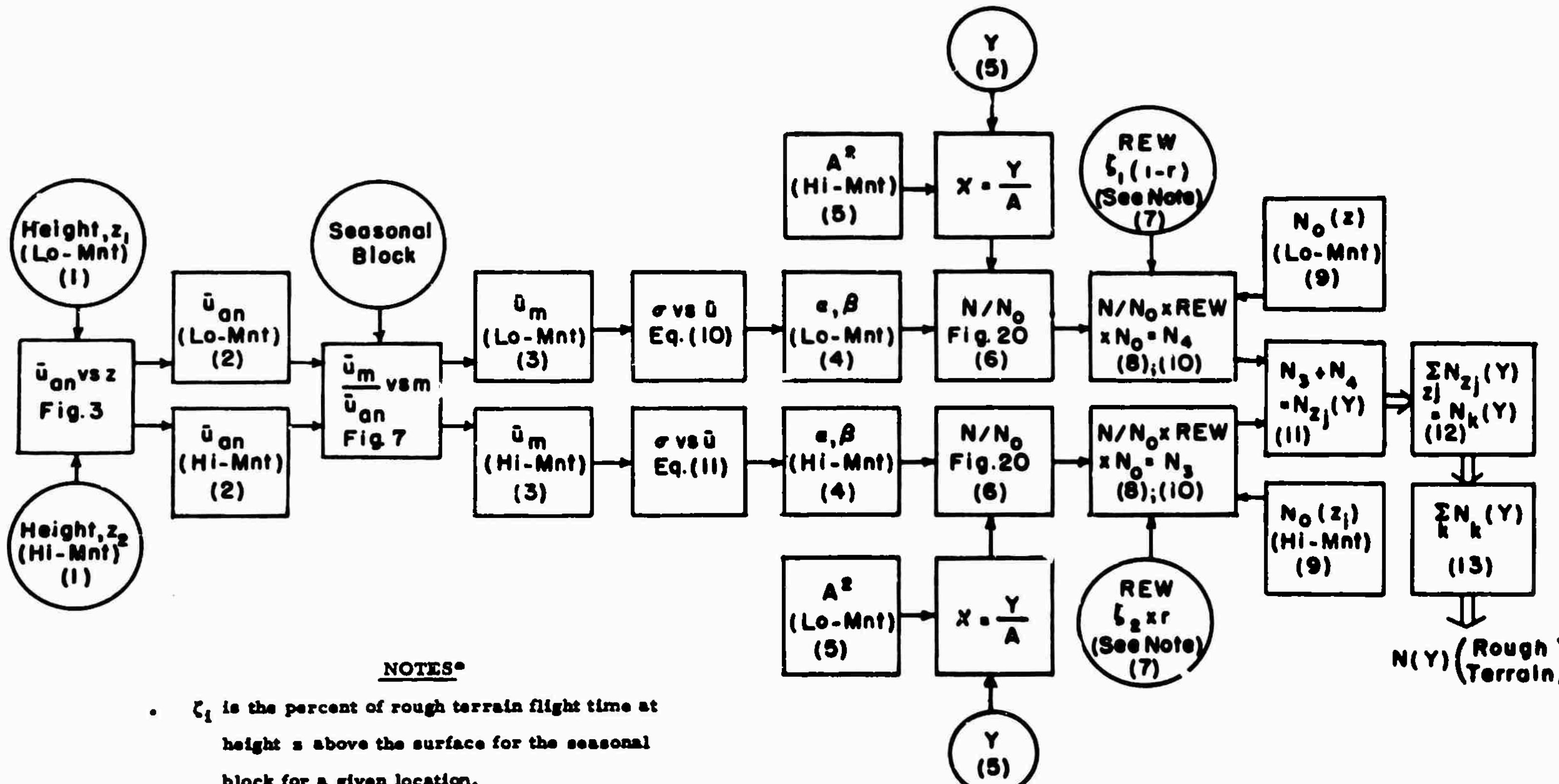

NOTES*

- ζ_i is the percent of rough terrain flight time at height z above the surface for the seasonal block for a given location.
- r is the percent of rough terrain flight time over high mountain terrain; (1 - r) the percent time over low mountain terrain.

Numbers in parenthesis refer to steps described in Section 8.

FIG. 22. FLOW CHART OF MODEL APPLICATION FOR ROUGH TERRAIN CONDITION.

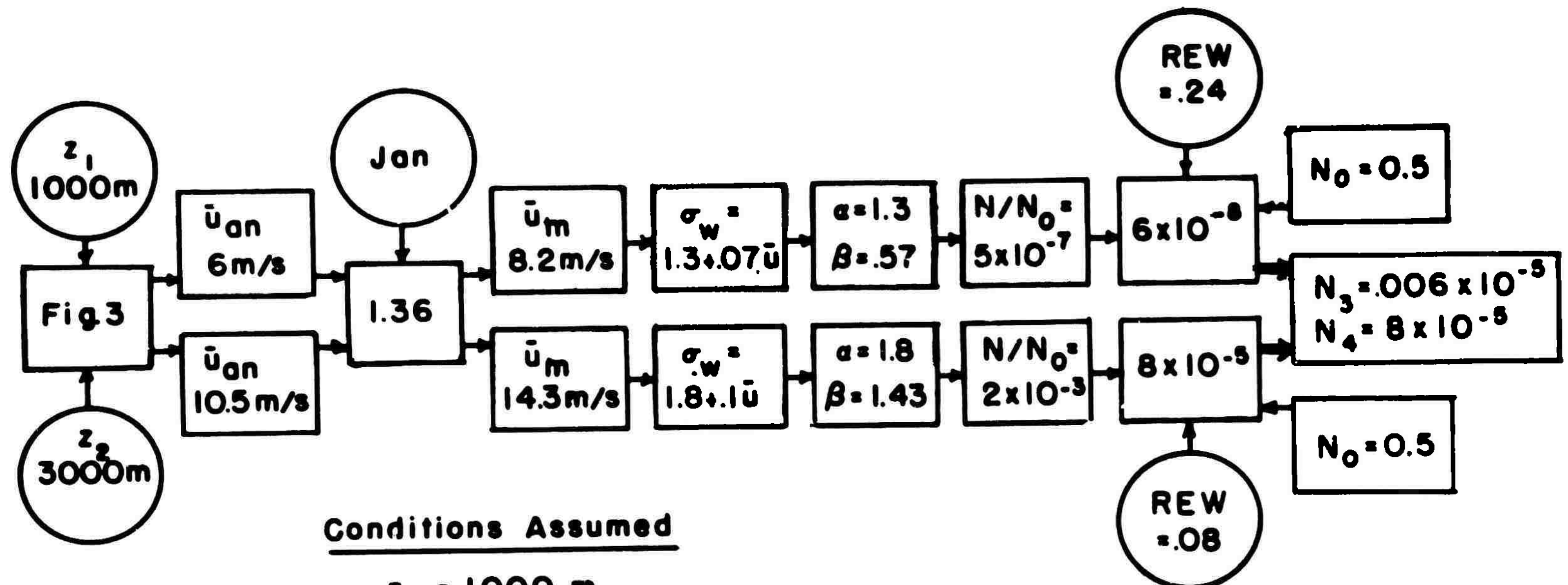

Conditions Assumed

z_1 = 1000 m

z_2 = 3000 m

m = January

Y/A = 14

ζ_1 = .4, ζ_2 = .2

r = .4

N_0 = 0.5

FIG. 23. FLOW CHART OF MODEL APPLICATION FOR SPECIFIED ROUGH TERRAIN CONDITIONS.

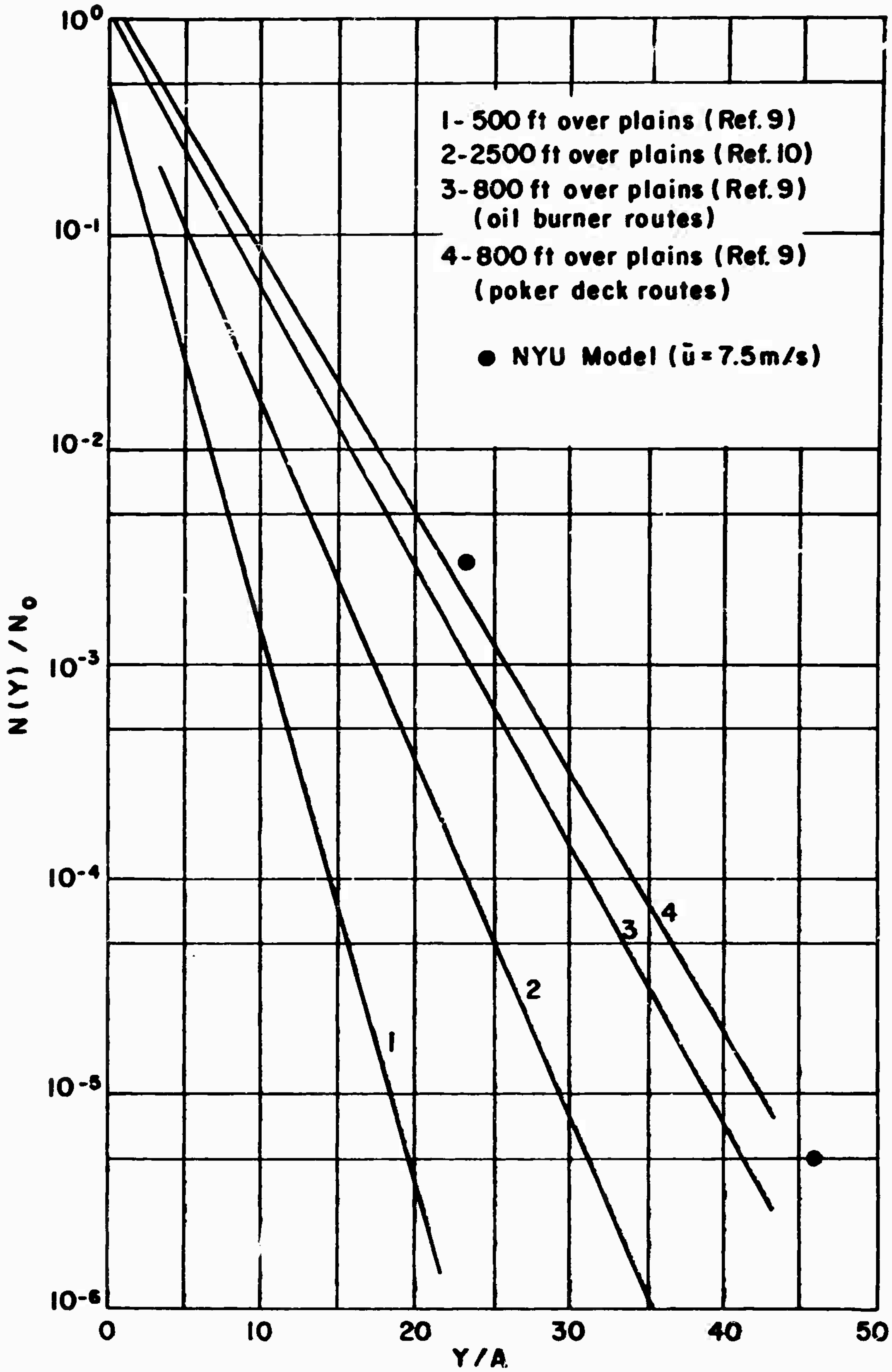

FIG. 24. A ROUGH COMPARISON OF B-52 CUMULATIVE LOAD EXCEEDANCE DATA AND NYU MODEL ESTIMATES.

UNCLASSIFIED

Security Classification

DOCUMENT CONTROL DATA - R&D

(Security classification of title, body of abstract and indexing annotation must be entered when the overall report is classified)

1. ORIGINATING ACTIVITY (Corporate author)

New York University
Geophysical Sciences Laboratory
2455 Sedgwick Avenue, Bronx, New York 10468

2a. REPORT SECURITY CLASSIFICATION: Unclassified

2b. GROUP

3. REPORT TITLE

A CLIMATOLOGICAL-WIND TURBULENCE MODEL FOR ESTIMATING LOW ALTITUDE GUST LOADS

4. DESCRIPTIVE NOTES (Type of report and inclusive dates)

Final Report, 15 April 1965 to 15 October 1966

5. AUTHOR(S) (Last name, first name, initial)

Lappe, U. Oscar

6. REPORT DATE	7a. TOTAL NO. OF PAGES	7b. NO. OF REFS
January 1968	63	11

8a. CONTRACT OR GRANT NO. AF 33(615)-2566

b. PROJECT NO. 1367

c. Task No. 136702

d.

9a. ORIGINATOR'S REPORT NUMBER(S): AFFDL-TR-67-122

9b. OTHER REPORT NO(S) (Any other numbers that may be assigned this report): GSL 66-13

10. AVAILABILITY/LIMITATION NOTICES

This document is subject to specific export controls and each transmittal to foreign governments or foreign nations may be made only with prior approval of AFFDL (FDTR), Wright-Patterson AFB, Ohio 45433.

11. SUPPLEMENTARY NOTES

12. SPONSORING MILITARY ACTIVITY

AFFDL (FDTR)
Wright-Patterson AFB, Ohio

13. ABSTRACT

The final phase in the development of a low altitude turbulence model for aircraft gust load application is described. The basic data used for this model are the B-66B low-level gust data and climatological wind data provided by the National Weather Records Center, Asheville, N. C. In preceding studies the turbulence spectrum functions, rms gust velocity/mean wind speed functions, and mean wind speed distribution functions were determined for variations in height, atmospheric stability, and terrain roughness conditions. In this final study needed to complete the turbulence model, climatological wind statistics are used to relate average mean wind speed characteristics to terrain, height, thermal stability, time of day and seasonal variations. The data represent locations throughout the United States. Based on results obtained from the climatological wind statistics, procedures are outlined for applying the turbulence model to estimate aircraft gust load exceedances for a specified low altitude operational history. A preliminary comparison of the model and B-52 service load data is made for an 800 ft terrain-clearance altitude.

DD FORM 1 JAN 64 1473

UNCLASSIFIED

Security Classification